and B*5801-expressing hosts harbored the Gag T242N escape mutation in the TW10 epitope and that the RCs of these strains correlated significantly with the accumulation of known and putative compensatory mutations in the capsid protein. Together with previously reported data from mutagenesis studies (10), these findings indicate that the accumulation of secondary mutations restores the fitness defects associated with primary escape mutations in a dose-dependent manner.

Despite a complex mixture of CTL escape and compensatory mutations present in chronic viral sequences, we observed a modest negative correlation between Gag-Protease function and CD4 T-cell count, which was strengthened upon restriction to protective HLA alleles only. Although these analyses are derived from cross-sectional data, results suggest that viral RC increases concomitantly as CD4 cell counts decline over the course of chronic infection. Indeed, the stronger correlations observed when analyses were restricted to protective HLA alleles suggest that changes in RC are greater over the course of chronic disease in the context of these alleles. This interpretation is consistent with our observation of a reduced RC in acute/early infection of individuals expressing protective HLA alleles, which is followed by an accumulation of compensatory changes that rescue the fitness costs of primary escape mutations. Unfortunately, we cannot fully explore this hypothesis, since infection dates are unknown for the chronic infection cohort. Efforts to examine RCs using longitudinal samples from well-characterized seroconverter cohorts will be necessary to address these issues further. Importantly, however, the fact that individuals with protective alleles exhibit reduced viral loads in chronic infection compared to those of their non-protective-allele-expressing counterparts strongly suggests that these early fitness hits, although no longer directly detectable at later time points due to the accumulation of compensatory mutations, may provide long-lasting beneficial effects.

The larger data set of recombinant viruses from chronically infected patients provided greater power to uncover specific amino acids in Gag and protease associated with RC. We identified 63 polymorphisms located at 40 codons in Gag and two polymorphisms located at codon 61 in protease that were independently associated with RC after correction for multiple comparisons ($q < 0.2$) (see Table S2 in the supplemental material). As seen for acute/early infection samples, the majority of these sites (22 of 42 sites) were previously associated with HLA-mediated selection (14), and many others lie within known CTL epitopes. However, few of these mutations matched the predominant HLA-associated polymorphisms identified in the published literature, possibly suggesting that less-common mutations at these sites are more likely to result in severe RC defects. Of interest, the strongest HLA associations with lower RCs in chronic infection were observed for HLA-A*31 and -B*40, and polymorphisms targeted by these alleles were also identified, namely, F383T (A*31) and E482D (B*40). Future studies will be necessary to examine the impact of these specific mutations on Gag RC and to assess their potential relevance for disease progression.

Polymorphisms at Gag codons 67, 218, 479, and 486 were associated with RC in both acute/early and chronic viruses. Of these polymorphisms, the S67A, V218X (acute/early) or V218Q (chronic), and L486X (acute/early) or L486S (chronic) mutations appeared to attenuate Gag RC, but interpretation of these results proved complex. For example, Gag position 67 appears to be under opposing selection pressures by different HLA alleles at the population level: while HLA-C*03 selects for S67A, HLA-A*02 selects for the wild-type serine at this residue (14). Mutations at codon 218 are associated with HLA-B*40, but this allele typically selects for alanine (rather than glutamine) at this residue (14). To our knowledge, mutations at codon 486 have not been identified as HLA footprints, although this residue lies within the known B*40-restricted KL9 epitope. Future site-directed mutagenesis studies will confirm these and other associations with viral RC so that they may be considered potential regions for inclusion or exclusion from Gag vaccine antigens designed to attenuate viral RC.

Several limitations of this study should be noted. First, we focused this work only on the Gag-Protease region of HIV-1. While we believe that the approach used provides a robust analysis of the impact of mutations in Gag and protease on the viral RC, we have not assessed important potential roles of polymorphisms located elsewhere in the viral genome. Second, due to the very large number of samples tested, we used bulk PCR products to construct recombinant viruses. The presence of amino acid mixtures in resulting stocks may have reduced our ability to detect minor differences in RC. Third, our acute/early infection study was limited to 66 individuals. This number was sufficient to observe a strong effect of protective HLA alleles on acute/early RC, but substantially larger acute/early infection cohorts may yield the ability to investigate RC associations with individual alleles and/or viral polymorphisms in greater detail.

In conclusion, this study and our previous report (64) focusing on subtype C infection represent the first systematic, population-based investigations of the contribution of HLA class I selection pressure on HIV-1 RC. Taken together, our findings are consistent with a model whereby HLA-associated CTL responses select for primary escape mutations in Gag during acute/early infection, some of which occur at a substantial fitness cost. Negative consequences for RC may be cumulative as additional escape mutations are selected; however, compensatory mutations that restore Gag function may also arise over extended periods of time. By late chronic infection, due to a balance of escape and compensatory mutations, many HLA-associated fitness defects observed during early infection are no longer detectable. A significant positive correlation between RC and the presence of compensatory mutations in chronic viruses illustrates the profound ability of continued *in vivo* viral evolution to rescue fitness defects. Nevertheless, the fact that individuals with protective alleles maintain lower pVLs than their non-protective-allele-expressing counterparts well into chronic infection strongly suggests that these early fitness hits may provide long-lasting benefits. These data provide important new information to better understand the complex interactions between HLA-mediated immune pressure and HIV-1 sequence evolution, the impact of escape and compensatory mutations on HIV-1 RC, and the potential utility of targeting attenuation-inducing sites in Gag for the rational design of an effective vaccine.

ACKNOWLEDGMENTS

We thank Brian Block, Celia Chui, Chelsea McCullough, Winnie Dong, David Knapp, Theresa Mo, and Jenna Spring for technical

assistance and Jenna Rychert for assistance with sample identification. Acute/early-infected patients were recruited through the Acute Infection and Early Disease Research Program (AIEDRP) network from sites in the United States and the National Centre in HIV Epidemiology and Clinical Research (NCHECR) Primary Infection Network in Sydney, Australia, by Robert Finlayson (Taylor Square Clinic, Darlinghurst) and Robert MacFarland (East Sydney Doctors, Darlinghurst).

This project was supported by grants from the Canadian Institutes for Health Research (CIHR) (to Z.L.B. and M.A.B.), the National Institutes of Health (grants AI028568, AI030914, AI074415, AI054178, and AI071915) (to B.D.W., T.M.A., M.A., and E.R.), the Howard Hughes Medical Institute, the Bill and Melinda Gates Foundation (to B.D.W. and T.M.A.), and the Harvard University Center for AIDS Research. Z.L.B. is a CIHR New Investigator Award recipient. C.J.B. is supported by an NSERC Julie Payette graduate scholarship. A.D.K. is supported by a program grant and practitioner fellowship from the Australian National Health and Medical Research Council. The NCHECR is supported by the Australian Commonwealth Department of Health and Ageing.

The funders had no role in study design, data collection and analysis, decision to publish, or preparation of the manuscript. The opinions expressed here are solely the responsibility of the authors and do not necessarily represent those held by their respective institutions or funding agencies.

M.A.B., Z.L.B., T.M., B.D.W., and T.M.A. designed this study. M.A.B, Z.L.B., J.S., P.C.R, and T.J.M. conducted experiments and analyzed data. C.J.B., C.M.K., J.M.C., and D.H. developed statistical methods and/or contributed to data analysis. H.S., A.D.K., H.J., E.R., M.M., M.A., and P.R.H. contributed specimens and/or clinical data. The manuscript was written by M.A.B. and Z.L.B. and critically reviewed by C.J.B., T.M., T.J.M., H.S., A.D.K., M.M., H.J., E.R., M.A., P.R.H., B.D.W., and T.M.A.

REFERENCES

1. **Allen, T. M., and M. Altfeld.** 2008. Crippling HIV one mutation at a time. J. Exp. Med. **205:**1003–1007.
2. **Allen, T. M., D. H. O'Connor, P. Jing, J. L. Dzuris, B. R. Mothe, T. U. Vogel, E. Dunphy, M. E. Liebl, C. Emerson, N. Wilson, K. J. Kunstman, X. Wang, D. B. Allison, A. L. Hughes, R. C. Desrosiers, J. D. Altman, S. M. Wolinsky, A. Sette, and D. I. Watkins.** 2000. Tat-specific cytotoxic T lymphocytes select for SIV escape variants during resolution of primary viraemia. Nature **407:** 386–390.
3. **Avila-Rios, S., C. E. Ormsby, J. M. Carlson, H. Valenzuela-Ponce, J. Blanco-Heredia, D. Garrido-Rodriguez, C. Garcia-Morales, D. Heckerman, Z. L. Brumme, S. Mallal, M. John, E. Espinosa, and G. Reyes-Teran.** 2009. Unique features of HLA-mediated HIV evolution in a Mexican cohort: a comparative study. Retrovirology **6:**72.
4. **Barouch, D. H., K. L. O'Brien, N. L. Simmons, S. L. King, P. Abbink, L. F. Maxfield, Y. H. Sun, A. La Porte, A. M. Riggs, D. M. Lynch, S. L. Clark, K. Backus, J. R. Perry, M. S. Seaman, A. Carville, K. G. Mansfield, J. J. Szinger, W. Fischer, M. Muldoon, and B. Korber.** 2010. Mosaic HIV-1 vaccines expand the breadth and depth of cellular immune responses in rhesus monkeys. Nat. Med. **16:**319–323.
5. **Barrie, K. A., E. E. Perez, S. L. Lamers, W. G. Farmerie, B. M. Dunn, J. W. Sleasman, and M. M. Goodenow.** 1996. Natural variation in HIV-1 protease, Gag p7 and p6, and protease cleavage sites within gag/pol polyproteins: amino acid substitutions in the absence of protease inhibitors in mothers and children infected by human immunodeficiency virus type 1. Virology **219:** 407–416.
6. **Borrow, P., H. Lewicki, B. H. Hahn, G. M. Shaw, and M. B. Oldstone.** 1994. Virus-specific CD8+ cytotoxic T-lymphocyte activity associated with control of viremia in primary human immunodeficiency virus type 1 infection. J. Virol. **68:**6103–6110.
7. **Borrow, P., H. Lewicki, X. Wei, M. S. Horwitz, N. Peffer, H. Meyers, J. A. Nelson, J. E. Gairin, B. H. Hahn, M. B. Oldstone, and G. M. Shaw.** 1997. Antiviral pressure exerted by HIV-1-specific cytotoxic T lymphocytes (CTLs) during primary infection demonstrated by rapid selection of CTL escape virus. Nat. Med. **3:**205–211.
8. **Boutwell, C. L., and M. Essex.** 2007. Identification of HLA class I-associated amino acid polymorphisms in the HIV-1C proteome. AIDS Res. Hum. Retroviruses **23:**165–174.
9. **Boutwell, C. L., C. F. Rowley, and M. Essex.** 2009. Reduced viral replication capacity of human immunodeficiency virus type 1 subtype C caused by cytotoxic-T-lymphocyte escape mutations in HLA-B57 epitopes of capsid protein. J. Virol. **83:**2460–2468.
10. **Brockman, M. A., A. Schneidewind, M. Lahaie, A. Schmidt, T. Miura, I. Desouza, F. Ryvkin, C. A. Derdeyn, S. Allen, E. Hunter, J. Mulenga, P. A. Goepfert, B. D. Walker, and T. M. Allen.** 2007. Escape and compensation from early HLA-B57-mediated cytotoxic T-lymphocyte pressure on human immunodeficiency virus type 1 Gag alter capsid interactions with cyclophilin A. J. Virol. **81:**12608–12618.
11. **Brumme, Z. L., C. J. Brumme, J. Carlson, H. Streeck, M. John, Q. Eichbaum, B. L. Block, B. Baker, C. Kadie, M. Markowitz, H. Jessen, A. D. Kelleher, E. Rosenberg, J. Kaldor, Y. Yuki, M. Carrington, T. M. Allen, S. Mallal, M. Altfeld, D. Heckerman, and B. D. Walker.** 2008. Marked epitope and allele-specific differences in rates of mutation in HIV-1 Gag, Pol and Nef CTL epitopes in acute/early HIV-1 infection. J. Virol. **82:**9216–9227.
12. **Brumme, Z. L., C. J. Brumme, C. Chui, T. Mo, B. Wynhoven, C. K. Woods, B. M. Henrick, R. S. Hogg, J. S. Montaner, and P. R. Harrigan.** 2007. Effects of human leukocyte antigen class I genetic parameters on clinical outcomes and survival after initiation of highly active antiretroviral therapy. J. Infect. Dis. **195:**1694–1704.
13. **Brumme, Z. L., C. J. Brumme, D. Heckerman, B. T. Korber, M. Daniels, J. Carlson, C. Kadie, T. Bhattacharya, C. Chui, J. Szinger, T. Mo, R. S. Hogg, J. S. Montaner, N. Frahm, C. Brander, B. D. Walker, and P. R. Harrigan.** 2007. Evidence of differential HLA class I-mediated viral evolution in functional and accessory/regulatory genes of HIV-1. PLoS Pathog. **3:**e94.
14. **Brumme, Z. L., M. John, J. M. Carlson, C. J. Brumme, D. Chan, M. A. Brockman, L. C. Swenson, I. Tao, S. Szeto, P. Rosato, J. Sela, C. M. Kadie, N. Frahm, C. Brander, D. W. Haas, S. Riddler, R. Haubrich, B. D. Walker, P. R. Harrigan, D. Heckerman, and S. Mallal.** 2009. HLA-associated immune escape pathways in HIV-1 subtype B Gag, Pol and Nef proteins. PLoS One **4:**e6687.
15. **Carlson, J. M., Z. L. Brumme, C. M. Rousseau, C. J. Brumme, P. Matthews, C. Kadie, J. I. Mullins, B. D. Walker, P. R. Harrigan, P. J. Goulder, and D. Heckerman.** 2008. Phylogenetic dependency networks: inferring patterns of CTL escape and codon covariation in HIV-1 Gag. PLoS Comput. Biol. **4:**e1000225.
16. **Carrington, M., and S. J. O'Brien.** 2003. The influence of HLA genotype on AIDS. Annu. Rev. Med. **54:**535–551.
17. **Chopera, D. R., Z. Woodman, K. Mlisana, M. Mlotshwa, D. P. Martin, C. Seoighe, F. Treurnicht, D. A. de Rosa, W. Hide, S. A. Karim, C. M. Gray, and C. Williamson.** 2008. Transmission of HIV-1 CTL escape variants provides HLA-mismatched recipients with a survival advantage. PLoS Pathog. **4:**e1000033.
18. **Couillin, I., B. Culmann-Penciolelli, E. Gomard, J. Choppin, J. P. Levy, J. G. Guillet, and S. Saragosti.** 1994. Impaired cytotoxic T lymphocyte recognition due to genetic variations in the main immunogenic region of the human immunodeficiency virus 1 NEF protein. J. Exp. Med. **180:**1129–1134.
19. **Crawford, H., W. Lumm, A. Leslie, M. Schaefer, D. Boeras, J. G. Prado, J. Tang, P. Farmer, T. Ndung'u, S. Lakhi, J. Gilmour, P. Goepfert, B. D. Walker, R. Kaslow, J. Mulenga, S. Allen, P. J. Goulder, and E. Hunter.** 2009. Evolution of HLA-B*5703 HIV-1 escape mutations in HLA-B*5703-positive individuals and their transmission recipients. J. Exp. Med. **206:**909–921.
20. **Crawford, H., J. G. Prado, A. Leslie, S. Hue, I. Honeyborne, S. Reddy, M. van der Stok, Z. Mncube, C. Brander, C. Rousseau, J. I. Mullins, R. Kaslow, P. Goepfert, S. Allen, E. Hunter, J. Mulenga, P. Kiepiela, B. D. Walker, and P. J. Goulder.** 2007. Compensatory mutation partially restores fitness and delays reversion of escape mutation within the immunodominant HLA-B*5703-restricted Gag epitope in chronic human immunodeficiency virus type 1 infection. J. Virol. **81:**8346–8351.
21. **Duda, A., L. Lee-Turner, J. Fox, N. Robinson, S. Dustan, S. Kaye, H. Fryer, M. Carrington, M. McClure, A. R. McLean, S. Fidler, J. Weber, R. E. Phillips, and A. J. Frater.** 2009. HLA-associated clinical progression correlates with epitope reversion rates in early human immunodeficiency virus infection. J. Virol. **83:**1228–1239.
22. **Edwards, B. H., A. Bansal, S. Sabbaj, J. Bakari, M. J. Mulligan, and P. A. Goepfert.** 2002. Magnitude of functional CD8+ T-cell responses to the gag protein of human immunodeficiency virus type 1 correlates inversely with viral load in plasma. J. Virol. **76:**2298–2305.
23. **Fiebig, E. W., D. J. Wright, B. D. Rawal, P. E. Garrett, R. T. Schumacher, L. Peddada, C. Heldebrant, R. Smith, A. Conrad, S. H. Kleinman, and M. P. Busch.** 2003. Dynamics of HIV viremia and antibody seroconversion in plasma donors: implications for diagnosis and staging of primary HIV infection. AIDS **17:**1871–1879.
24. **Friedrich, T. C., E. J. Dodds, L. J. Yant, L. Vojnov, R. Rudersdorf, C. Cullen, D. T. Evans, R. C. Desrosiers, B. R. Mothe, J. Sidney, A. Sette, K. Kunstman, S. Wolinsky, M. Piatak, J. Lifson, A. L. Hughes, N. Wilson, D. H. O'Connor, and D. I. Watkins.** 2004. Reversion of CTL escape-variant immunodeficiency viruses in vivo. Nat. Med. **10:**275–281.
25. **Gao, X., A. Bashirova, A. K. Iversen, J. Phair, J. J. Goedert, S. Buchbinder, K. Hoots, D. Vlahov, M. Altfeld, S. J. O'Brien, and M. Carrington.** 2005. AIDS restriction HLA allotypes target distinct intervals of HIV-1 pathogenesis. Nat. Med. **11:**1290–1292.
26. **Gaschen, B., J. Taylor, K. Yusim, B. Foley, F. Gao, D. Lang, V. Novitsky, B. Haynes, B. H. Hahn, T. Bhattacharya, and B. Korber.** 2002. Diversity considerations in HIV-1 vaccine selection. Science **296:**2354–2360.
27. **Goepfert, P. A., W. Lumm, P. Farmer, P. Matthews, A. Prendergast, J. M. Carlson, C. A. Derdeyn, J. Tang, R. A. Kaslow, A. Bansal, K. Yusim, D.**

Heckerman, J. Mulenga, S. Allen, P. J. Goulder, and E. Hunter. 2008. Transmission of HIV-1 Gag immune escape mutations is associated with reduced viral load in linked recipients. J. Exp. Med. **205:**1009–1017.

28. **Goonetilleke, N., M. K. Liu, J. F. Salazar-Gonzalez, G. Ferrari, E. Giorgi, V. V. Ganusov, B. F. Keele, G. H. Learn, E. L. Turnbull, M. G. Salazar, K. J. Weinhold, S. Moore, N. Letvin, B. F. Haynes, M. S. Cohen, P. Hraber, T. Bhattacharya, P. Borrow, A. S. Perelson, B. H. Hahn, G. M. Shaw, B. T. Korber, and A. J. McMichael.** 2009. The first T cell response to transmitted/founder virus contributes to the control of acute viremia in HIV-1 infection. J. Exp. Med. **206:**1253–1272.
29. **Goulder, P. J., R. E. Phillips, R. A. Colbert, S. McAdam, G. Ogg, M. A. Nowak, P. Giangrande, G. Luzzi, B. Morgan, A. Edwards, A. J. McMichael, and S. Rowland-Jones.** 1997. Late escape from an immunodominant cytotoxic T-lymphocyte response associated with progression to AIDS. Nat. Med. **3:**212–217.
30. **Guindon, S., and O. Gascuel.** 2003. A simple, fast, and accurate algorithm to estimate large phylogenies by maximum likelihood. Syst. Biol. **52:**696–704.
31. **Honeyborne, I., A. Prendergast, F. Pereyra, A. Leslie, H. Crawford, R. Payne, S. Reddy, K. Bishop, E. Moodley, K. Nair, M. van der Stok, N. McCarthy, C. M. Rousseau, M. Addo, J. I. Mullins, C. Brander, P. Kiepiela, B. D. Walker, and P. J. Goulder.** 2007. Control of human immunodeficiency virus type 1 is associated with HLA-B*13 and targeting of multiple gag-specific CD8+ T-cell epitopes. J. Virol. **81:**3667–3672.
32. **Huang, X., and J. Zhang.** 1996. Methods for comparing a DNA sequence with a protein sequence. Comput. Appl. Biosci. **12:**497–506.
33. **Janssen, R. S., G. A. Satten, S. L. Stramer, B. D. Rawal, T. R. O'Brien, B. J. Weiblen, F. M. Hecht, N. Jack, F. R. Cleghorn, J. O. Kahn, M. A. Chesney, and M. P. Busch.** 1998. New testing strategy to detect early HIV-1 infection for use in incidence estimates and for clinical and prevention purposes. JAMA **280:**42–48.
34. **John, M., D. Heckerman, I. James, L. P. Park, J. M. Carlson, A. Chopra, S. Gaudieri, D. Nolan, D. Haas, S. A. Riddler, D. Haubrich, and S. Mallal.** 2010. Adaptive interactions between HLA and HIV-1: highly divergent selection imposed by HLA class I molecules with common supertype motifs. J. Immunol. **184:**4368–4377.
35. **Kelleher, A. D., C. Long, E. C. Holmes, R. L. Allen, J. Wilson, C. Conlon, C. Workman, S. Shaunak, K. Olson, P. Goulder, C. Brander, G. Ogg, J. S. Sullivan, W. Dyer, I. Jones, A. J. McMichael, S. Rowland-Jones, and R. E. Phillips.** 2001. Clustered mutations in HIV-1 gag are consistently required for escape from HLA-B27-restricted cytotoxic T lymphocyte responses. J. Exp. Med. **193:**375–386.
36. **Kiepiela, P., K. Ngumbela, C. Thobakgale, D. Ramduth, I. Honeyborne, E. Moodley, S. Reddy, C. de Pierres, Z. Mncube, N. Mkhwanazi, K. Bishop, M. van der Stok, K. Nair, N. Khan, H. Crawford, R. Payne, A. Leslie, J. Prado, A. Prendergast, J. Frater, N. McCarthy, C. Brander, G. H. Learn, D. Nickle, C. Rousseau, H. Coovadia, J. I. Mullins, D. Heckerman, B. D. Walker, and P. Goulder.** 2007. CD8+ T-cell responses to different HIV proteins have discordant associations with viral load. Nat. Med. **13:**46–53.
37. **Koch, N., N. Yahi, J. Fantini, and C. Tamalet.** 2001. Mutations in HIV-1 gag cleavage sites and their association with protease mutations. AIDS **15:**526–528.
38. **Korber, B. T., N. L. Letvin, and B. F. Haynes.** 2009. T-cell vaccine strategies for human immunodeficiency virus, the virus with a thousand faces. J. Virol. **83:**8300–8314.
39. **Koup, R. A., J. T. Safrit, Y. Cao, C. A. Andrews, G. McLeod, W. Borkowsky, C. Farthing, and D. D. Ho.** 1994. Temporal association of cellular immune responses with the initial control of viremia in primary human immunodeficiency virus type 1 syndrome. J. Virol. **68:**4650–4655.
40. **Leslie, A. J., and P. J. Goulder.** 2006. HIV escape and attenuation by cytotoxic T lymphocytes. Curr. Opin. HIV AIDS **1:**34–39.
41. **Leslie, A. J., K. J. Pfafferott, P. Chetty, R. Draenert, M. M. Addo, M. Feeney, Y. Tang, E. C. Holmes, T. Allen, J. G. Prado, M. Altfeld, C. Brander, C. Dixon, D. Ramduth, P. Jeena, S. A. Thomas, A. St. John, T. A. Roach, B. Kupfer, G. Luzzi, A. Edwards, G. Taylor, H. Lyall, G. Tudor-Williams, V. Novelli, J. Martinez-Picado, P. Kiepiela, B. D. Walker, and P. J. Goulder.** 2004. HIV evolution: CTL escape mutation and reversion after transmission. Nat. Med. **10:**282–289.
42. **Martinez-Picado, J., J. G. Prado, E. E. Fry, K. Pfafferott, A. Leslie, S. Chetty, C. Thobakgale, I. Honeyborne, H. Crawford, P. Matthews, T. Pillay, C. Rousseau, J. I. Mullins, C. Brander, B. D. Walker, D. I. Stuart, P. Kiepiela, and P. Goulder.** 2006. Fitness cost of escape mutations in p24 Gag in association with control of human immunodeficiency virus type 1. J. Virol. **80:**3617–3623.
43. **Matthews, P. C., A. Prendergast, A. Leslie, H. Crawford, R. Payne, C. Rousseau, M. Rolland, I. Honeyborne, J. Carlson, C. Kadie, C. Brander, K. Bishop, N. Mlotshwa, J. D. Mullins, H. Coovadia, T. Ndung'u, B. D. Walker, D. Heckerman, and P. J. Goulder.** 2008. Central role of reverting mutations in HLA associations with human immunodeficiency virus set point. J. Virol. **82:**8548–8559.
44. **McMichael, A. J., P. Borrow, G. D. Tomaras, N. Goonetilleke, and B. F. Haynes.** 2010. The immune response during acute HIV-1 infection: clues for vaccine development. Nat. Rev. Immunol. **10:**11–23.
45. **McMichael, A. J., and R. E. Phillips.** 1997. Escape of human immunodeficiency virus from immune control. Annu. Rev. Immunol. **15:**271–296.
46. **Miura, T., M. A. Brockman, C. J. Brumme, Z. L. Brumme, J. M. Carlson, F. Pereyra, A. Trocha, M. M. Addo, B. L. Block, A. C. Rothchild, B. M. Baker, T. Flynn, A. Schneidewind, B. Li, Y. E. Wang, D. Heckerman, T. M. Allen, and B. D. Walker.** 2008. Genetic characterization of human immunodeficiency virus type 1 in elite controllers: lack of gross genetic defects or common amino acid changes. J. Virol. **82:**8422–8430.
47. **Miura, T., M. A. Brockman, Z. L. Brumme, C. J. Brumme, F. Pereyra, A. Trocha, B. L. Block, A. Schneidewind, T. M. Allen, D. Heckerman, and B. D. Walker.** 2009. HLA-associated alterations in replication capacity of chimeric NL4-3 viruses carrying gag-Protease from elite controllers of human immunodeficiency virus type 1. J. Virol. **83:**140–149.
48. **Miura, T., M. A. Brockman, A. Schneidewind, M. Lobritz, F. Pereyra, A. Rathod, B. L. Block, Z. L. Brumme, C. J. Brumme, B. Baker, A. C. Rothchild, B. Li, A. Trocha, E. Cutrell, N. Frahm, C. Brander, I. Toth, E. J. Arts, T. M. Allen, and B. D. Walker.** 2009. HLA-B57/B*5801 human immunodeficiency virus type 1 elite controllers select for rare gag variants associated with reduced viral replication capacity and strong cytotoxic T-lymphocyte recognition. J. Virol. **83:**2743–2755.
49. **Miura, T., Z. L. Brumme, M. Brockman, P. Rosato, J. Sela, C. J. Brumme, F. Pereyra, D. E. Kaufmann, A. Trocha, B. L. Block, E. S. Daar, E. Connick, H. Jessen, A. D. Kelleher, E. Rosenberg, M. Markowitz, K. Schafer, F. Vaida, A. Iwamoto, S. Little, and B. D. Walker.** 2010. Impaired replication capacity of acute/early viruses in persons who become HIV controllers. J. Virol. **84:**7581–7591.
50. **Moore, C. B., M. John, I. R. James, F. T. Christiansen, C. S. Witt, and S. A. Mallal.** 2002. Evidence of HIV-1 adaptation to HLA-restricted immune responses at a population level. Science **296:**1439–1443.
51. **O'Brien, S. J., X. Gao, and M. Carrington.** 2001. HLA and AIDS: a cautionary tale. Trends Mol. Med. **7:**379–381.
52. **Peyerl, F. W., H. S. Bazick, M. H. Newberg, D. H. Barouch, J. Sodroski, and N. L. Letvin.** 2004. Fitness costs limit viral escape from cytotoxic T lymphocytes at a structurally constrained epitope. J. Virol. **78:**13901–13910.
53. **Prado, J. G., I. Honeyborne, I. Brierley, M. C. Puertas, J. Martinez-Picado, and P. J. Goulder.** 2009. Functional consequences of human immunodeficiency virus escape from an HLA-B*13-restricted CD8+ T-cell epitope in p1 Gag protein. J. Virol. **83:**1018–1025.
54. **Price, D. A., P. J. Goulder, P. Klenerman, A. K. Sewell, P. J. Easterbrook, M. Troop, C. R. Bangham, and R. E. Phillips.** 1997. Positive selection of HIV-1 cytotoxic T lymphocyte escape variants during primary infection. Proc. Natl. Acad. Sci. U. S. A. **94:**1890–1895.
55. **Rolland, M., D. C. Nickle, and J. I. Mullins.** 2007. HIV-1 group M conserved elements vaccine. PLoS Pathog. **3:**e157.
56. **Rousseau, C. M., M. G. Daniels, J. M. Carlson, C. Kadie, H. Crawford, A. Prendergast, P. Matthews, R. Payne, M. Rolland, D. N. Raugi, B. S. Maust, G. H. Learn, D. C. Nickle, H. Coovadia, T. Ndung'u, N. Frahm, C. Brander, B. D. Walker, P. J. Goulder, T. Bhattacharya, D. E. Heckerman, B. T. Korber, and J. I. Mullins.** 2008. HLA class I-driven evolution of human immunodeficiency virus type 1 subtype C proteome: immune escape and viral load. J. Virol. **82:**6434–6446.
57. **Rowland-Jones, S. L., R. E. Phillips, D. F. Nixon, F. M. Gotch, J. P. Edwards, A. O. Ogunlesi, J. G. Elvin, J. A. Rothbard, C. R. Bangham, C. R. Rizza, et al.** 1992. Human immunodeficiency virus variants that escape cytotoxic T-cell recognition. AIDS Res. Hum. Retroviruses **8:**1353–1354.
58. **Schneidewind, A., M. A. Brockman, J. Sidney, Y. E. Wang, H. Chen, T. J. Suscovich, B. Li, R. I. Adam, R. L. Allgaier, B. R. Mothe, T. Kuntzen, C. Oniangue-Ndza, A. Trocha, X. G. Yu, C. Brander, A. Sette, B. D. Walker, and T. M. Allen.** 2008. Structural and functional constraints limit options for cytotoxic T-lymphocyte escape in the immunodominant HLA-B27-restricted epitope in human immunodeficiency virus type 1 capsid. J. Virol. **82:**5594–5605.
59. **Schneidewind, A., M. A. Brockman, R. Yang, R. I. Adam, B. Li, S. Le Gall, C. R. Rinaldo, S. L. Craggs, R. L. Allgaier, K. A. Power, T. Kuntzen, C. S. Tung, M. X. LaBute, S. M. Mueller, T. Harrer, A. J. McMichael, P. J. Goulder, C. Aiken, C. Brander, A. D. Kelleher, and T. M. Allen.** 2007. Escape from the dominant HLA-B27-restricted cytotoxic T-lymphocyte response in Gag is associated with a dramatic reduction in human immunodeficiency virus type 1 replication. J. Virol. **81:**12382–12393.
60. **Storey, J. D., and R. Tibshirani.** 2003. Statistical significance for genomewide studies. Proc. Natl. Acad. Sci. U. S. A. **100:**9440–9445.
61. **Taylor, B. S., and S. M. Hammer.** 2008. The challenge of HIV-1 subtype diversity. N. Engl. J. Med. **359:**1965–1966.
62. **Troyer, R. M., J. McNevin, Y. Liu, S. C. Zhang, R. W. Krizan, A. Abraha, D. M. Tebit, H. Zhao, S. Avila, M. A. Lobritz, M. J. McElrath, S. Le Gall, J. I. Mullins, and E. J. Arts.** 2009. Variable fitness impact of HIV-1 escape mutations to cytotoxic T lymphocyte (CTL) response. PLoS Pathog. **5:**e1000365.
63. **Wang, Y. E., B. Li, J. M. Carlson, H. Streeck, A. D. Gladden, R. Goodman, A. Schneidewind, K. A. Power, I. Toth, N. Frahm, G. Alter, C. Brander, M. Carrington, B. D. Walker, M. Altfeld, D. Heckerman, and T. M. Allen.** 2009. Protective HLA class I alleles that restrict acute-phase CD8+ T-cell responses

are associated with viral escape mutations located in highly conserved regions of human immunodeficiency virus type 1. J. Virol. **83:**1845–1855.

64. **Wright, J. K., Z. L. Brumme, J. M. Carlson, D. Heckerman, C. M. Kadie, C. J. Brumme, B. Wang, E. Losina, T. Miura, F. Chonco, M. van der Stok, Z. Mncube, K. Bishop, P. J. R. Goulder, B. D. Walker, M. A. Brockman, and T. Ndung'u.** 2010. Gag-Protease-mediated replication capacity in HIV-1 subtype C chronic infection: associations with HLA type and clinical parameters. J. Virol. **84:**10820–10831.
65. **Yeh, W. W., E. M. Cale, P. Jaru-Ampornpan, C. I. Lord, F. W. Peyerl, and N. L. Letvin.** 2006. Compensatory substitutions restore normal core assembly in simian immunodeficiency virus isolates with Gag epitope cytotoxic T-lymphocyte escape mutations. J. Virol. **80:**8168–8177.
66. **Zuniga, R., A. Lucchetti, P. Galvan, S. Sanchez, C. Sanchez, A. Hernandez, H. Sanchez, N. Frahm, C. H. Linde, H. S. Hewitt, W. Hildebrand, M. Altfeld, T. M. Allen, B. D. Walker, B. T. Korber, T. Leitner, J. Sanchez, and C. Brander.** 2006. Relative dominance of Gag p24-specific cytotoxic T lymphocytes is associated with human immunodeficiency virus control. J. Virol. **80:**3122–3125.

Microbiology and Immunology

Microbiol Immunol 2010; 54: 734–746
doi:10.1111/j.1348-0421.2010.00276.x

ORIGINAL ARTICLE

Intracellular localization of human immunodeficiency virus type 1 Gag and GagPol products and virus particle release: relationship with the Gag-to-GagPol ratio

Hiyori Haraguchi[1], Sho Sudo[1], Takeshi Noda[2], Fumitaka Momose[1], Yoshihiro Kawaoka[2,3,4] and Yuko Morikawa[1]

[1]Graduate School for Infection Control, Kitasato University, Shirokane 5-9-1, Minato-ku, Tokyo 108-8641, [2]Institute of Medical Science, University of Tokyo, Shirokanedai 4-6-1, Minato-ku, Tokyo 108-8639, [3]Exploratory Research for Advanced Technology Infection-Induced Host Responses Project, Japan Science and Technology Agency, Saitama, Japan; and [4]Influenza Research Institute, Department of Pathological Sciences, University of Wisconsin-Madison, Madison, WI, USA

ABSTRACT

Human immunodeficiency virus (HIV) Gag precursor protein is cleaved by viral protease (PR) within GagPol precursor protein to produce the mature matrix (MA), capsid, nucleocapsid, and p6 domains. This processing is termed maturation and required for HIV infectivity. In order to understand the intracellular sites and mechanisms of HIV maturation, HIV molecular clones in which Gag and GagPol were tagged with FLAG and hemagglutinin epitope sequences at the C-termini, respectively were made. When coexpressed, both Gag and GagPol were incorporated into virus particles. Temporal analysis by confocal microscopy showed that Gag and GagPol were relocated from the cytoplasm to the plasma membrane. Mature cleaved MA was observed only at sites on the plasma membrane where both Gag and GagPol had accumulated, indicating that Gag processing occurs during Gag/GagPol assembly at the plasma membrane, but not during membrane trafficking. Fluorescence resonance energy transfer imaging suggested that these were the primary sites of GagPol dimerization. In contrast, with overexpression of GagPol alone an absence of particle release was observed, and this was associated with diffuse distribution of mature cleaved MA throughout the cytoplasm. Alteration of the Gag-to-GagPol ratio similarly impaired virus particle release with aberrant distributions of mature MA in the cytoplasm. However, when PR was inactive, it seemed that the Gag-to-GagPol ratio was not critical for virus particle release but virus particles encasing unusually large numbers of GagPol molecules were produced, these particles displaying aberrant virion morphology. Taken together, it was concluded that the Gag-to-GagPol ratio has significant impacts on either intracellular distributions of mature cleaved MA or the morphology of virus particles produced.

Key words GagPol, HIV-1, plasma membrane, ratio.

Human immunodeficiency virus (HIV) contains three viral structural proteins: Gag, GagPol, and Env. Gag protein, the main structural component of HIV particles, is synthesized in the cytosol as a 55 kDa precursor protein and is targeted to the cellular membrane, where virus particle budding occurs. During translation of Gag mRNA, ribosomal frameshifting occurs at an efficiency of 5–10% and generates a 160 kDa GagPol fusion protein at a 10–20:1 ratio of Gag to GagPol (1). Following protein synthesis, Gag and GagPol proteins are relocated to the membrane

Correspondence
Yuko Morikawa, Graduate School for Infection Control, Kitasato University, Shirokane 5-9-1, Minato-ku, Tokyo 108-8641, Japan.
Tel: +81 3 5791 6129; fax: +81 3 5791 6268; email: morikawa@lisci.kitasato-u.ac.jp

Received 10 August 2010; revised 28 September 2010; accepted 1 October 2010.

List of Abbreviations: CA, capsid; EGFP, enhanced green fluorescent protein; FRET, fluorescence resonance energy transfer; GFP, green fluorescent protein; HA, hemagglutinin; HIV, Human immunodeficiency virus; IN, integrase; MA, matrix; NC, nucleocapsid; PR, protease; RT, reverse transcriptase; WT, wild-type.

and co-assembled into virus particles. Although HIV particle assembly is essentially directed by Gag protein (2, 3) and GagPol protein is only incorporated into virus particles through co-assembly with Gag (4, 5), the incorporation of GagPol into virus particles is crucial for virion infectivity, since the Pol region harbors virus-specific enzymes, PR, RT, and IN, all of which are essential for HIV replication.

Concomitant with the incorporation of GagPol protein, Gag protein undergoes a process termed maturation in which it is cleaved by PR located in GagPol to produce mature p17/MA, p24/CA, p7/NC, and p6 domains, and p1 and p2 spacer peptides (6). Expression of the intact GagPol region produces a mature form of virus particle, which displays an electron-dense core encased in a conical capsid, whereas expression of Gag without the Pol region results in an immature form of virus particle, with a characteristic doughnut-like morphology (2, 5). A number of studies have shown that Gag expression with genetically engineered inactive PR fails to cleave Gag protein and results in production of virus particles that have been arrested at the immature stage (4, 7, 8). Since two forms of virus particles (immature and mature) have traditionally been observed for many retroviruses, retroviral maturation has been thought to take place at a very late stage of particle assembly, such as particle budding, or even after particle release (9). However, it is difficult to know when and where Gag processing takes place because mature virion morphology is only seen extracellularly, whereas Gag processing products are often observed in the cytoplasm.

Despite the obligatory role of active PR in HIV maturation, overexpression of GagPol fusion protein or an active PR domain induces enhancement of intracellular Gag processing, leading to a failure of particle production (10–12). These findings suggest that premature Gag processing in the cytoplasm can occur when the Gag-to-GagPol ratio is altered, and that the products of such premature processing may not participate in virus particle formation. Recent studies have also indicated that the Gag-to-GagPol ratio is important for virion RNA dimerization (13). Since the enzymatically active form of PR is a dimer, and the appearance of PR activity is accompanied by autoprocessing of PR from a GagPol precursor (14, 15), it is plausible that dimerization of GagPol precursors is a prerequisite for autoprocessing of PR. Timing of autoprocessing of the putative precursor dimer must be regulated for efficient particle production to occur in HIV infection. However, so far no studies have revealed the primary intracellular sites of Gag/GagPol processing or GagPol dimerization. The difficulties for such studies are: (i) discrimination between Gag and GagPol, because the N-terminal half of GagPol is identical with Gag, and (ii) discrimination between Gag/GagPol precursors and their processing products. To overcome these difficulties, we here added two distinct epitope tags (FLAG and HA) to the C-termini of Gag and GagPol, respectively, and immunostained with anti-HIV-1 p17/MA antibody, an antibody which recognizes the mature form of p17/MA but not uncleaved Gag precursors (16). Our confocal data demonstrated that Gag and GagPol were relocated from the cytoplasm to the plasma membrane and that Gag processing occurred only at sites in the plasma membrane where both Gag and GagPol had accumulated. Furthermore, we confirmed that these were the sites of GagPol dimerization by FRET imaging. Importantly, our data indicated that the failure of particle release caused by overexpression of GagPol could be explained by aberrant distribution of the mature p17/MA in the cytoplasm. Our study provides clues toward understanding the overall process of HIV maturation.

MATERIALS AND METHODS

Construction of HIV-1 molecular clones

In this study HIV-1 molecular clone pNL43 was used to construct its derivatives (17). An HIV molecular clone expressing an inactive form of PR has also been described previously (18). The FLAG and HA epitope sequences were added to the C-termini of Gag and GagPol proteins, respectively. For in-frame insertion of the FLAG sequence into the p6 region, overlapping PCR was carried out using a forward primer 5′-GATTACAAGGACGA CGACGACAAGAGACCAGAGCCAACAGCCCCAC-3′. Addition of the HA epitope tag sequence to the C-terminus of the *pol* gene was similarly carried out using a reverse primer 5′-GCTATGTCGACCATATGGCT AAGCGTAATCTGGAACATCGTATGGGTATCTAGAAT CCTCATCCTGTCTACTTGCCAC-3′. For expression of Gag without GagPol protein, two termination codons were introduced into the *pol* frame immediately downstream of the gag termination codon using 5′-CCCCTCGTCACAATAAAGTAAGGGGGGTAATTAAA GGAAGCTCTAT-3′ (termination codons in the *gag* and *pol* frames are underlined). For expression of GagPol protein alone, the *gag* and *pol* genes were placed into the same reading frame by deleting the 5T nucleotides at the frameshifting site (nucleotide positions 2086 to 2090). For FRET imaging, unique *XbaI* and *NotI* sites were initially introduced at the junction of PR/RT and the sequences encoding EGFP and Strawberry protein were inserted in-frame between the *XbaI* and *NotI* sites. The sequences encoding EGFP and Strawberry fluorescent protein were similarly added to the C-termini of Gag (for positive controls).

Cell culture and DNA transfection

HeLa cells were cultured in Dulbecco's modified Eagle's medium (Sigma, St Louis, MO, USA) supplemented with 10% FBS. DNA transfection was carried out using Lipofectamine 2000 (Invitrogen, Tokyo, Japan).

Western blotting

Following transfection, culture media were subjected to centrifugation through 20% (wt/vol) sucrose cushions at 120,000 × *g* for 2 hr at 4°C. Cells and virus particles were analyzed by Western blotting using anti-FLAG rabbit (Sigma), anti-HA mouse (Sigma), anti-HIV-1 RT mouse (ICN Pharmaceuticals, Cleveland, OH, USA), anti-HIV-1 p24/CA mouse (19), and anti-HIV-1 p17/MA mouse (Advanced Bio-technologies, Suwanee, GA, USA) antibodies. In some experiments, virus particles were further subjected to equilibrium centrifugation in 20–60% (wt/vol) sucrose gradients at 120,000 × *g* for 16 hr at 4°C and subjected to fractionation.

Confocal microscopy

HeLa cells were fixed with 3.7% paraformaldehyde in PBS for 30 min at room temperature, then permeabilized with 0.1% Triton X-100 for 5 min at room temperature. Following blocking, the cells were incubated with anti-FLAG mouse or rabbit (Sigma), anti-HA mouse or rabbit (Santa Cruz, Santa Crz, CA, USA), anti-HIV-1 RT mouse, and anti-HIV-1 p17/MA mouse antibodies, and subsequently with Alexa Fluor 488 or 568-conjugated anti-mouse and anti-rabbit antibodies (Molecular Probes, Eugene, OR, USA). Nuclear staining was carried out with TOPRO-3 (Molecular Probes) and the cells observed with a laser scanning confocal microscope (Leica, Heidelberg, Germany).

Electron microscopy

HeLa cells were fixed with 2.5% glutaraldehyde in 0.1 M cacodylate buffer (pH 7.4) for 1 hr at 4°C prior to treatment with 2% osmium tetroxide for 1 hr at 4°C. Ultrathin sections were stained with uranyl acetate and lead citrate and examined with an electron microscope (H-7500, Hitachi, Tokyo, Japan) at 80 kV.

Fluorescence resonance energy transfer imaging

HeLa cells were fixed with 3.7% paraformaldehyde in PBS for 30 min at room temperature and subjected to laser scanning confocal microscopy (Yokogawa, Sugar Land, TX, USA). Images were acquired using three filter combinations: EGFP excitation/EGFP emission (donor channel), Strawberry excitation/Strawberry emission (acceptor channel), and GFP excitation/Strawberry emission (FRET channel). FRET was confirmed by two changes in fluorescence signals upon photobleaching of the acceptor: (i) a decrease in donor fluorescence, and (ii) a proportional increase in acceptor fluorescence. Pixel by pixel analysis of FRET was carried out using the PixFRET plug-in of ImageJ software (20).

RESULTS

Addition of epitope tags had no detrimental effect on viral particle production

HIV-1 molecular clone pNL43 (17) is referred as WT in this study. To discriminate between Gag and GagPol proteins, we added FLAG and HA epitope tag sequences to the C-terminal regions of HIV-1 Gag and GagPol proteins, respectively (Fig. 1a). The Gag/GagPol constructs were introduced into pNL43. The C-terminal p6 domain of Gag has three functional motifs as follows. The first two, namely the PTAP and YPXnL sequences, are binding sites of tumor susceptibility gene 101 and ALG-2-interacting protein X/ALG-2-interacting protein 1, respectively, and both are required for particle budding (21–25). The third, the LXXLFG sequence, is a binding site of viral accessory protein Vpr (26, 27). The FLAG-tag sequence (DYKDDDDK) was inserted upstream of the PTAP sequence, in-frame in the p6 domain, which generated insertion of the RLQGRRRQE sequence in the *pol* frame. The HA-tag sequence was added to the C-terminus of the GagPol protein. The construct expressing both Gag-FLAG and GagPol-HA is referred to here as Gag-FLAG/Pol-HA. We also created a pNL43 derivative expressing GagPol-HA alone by deletion of the frameshift signal (referred to as GagPol-HA).

To assess the effect of the addition of the epitope tags, HeLa cells were transfected with the Gag-FLAG/Pol-HA construct, GagPol-HA construct, and its parental clone without the epitope tags, all of which are pNL43 derivatives containing inactive PR. Then, intracellular expression of Gag/GagPol proteins and particle production were examined by Western blotting using anti-HIV-1 p24/CA and anti-FLAG (for Gag protein) and anti-HIV-1 RT and anti-HA (for GagPol protein) antibodies (Fig. 1b). Gag-FLAG and GagPol-HA proteins were specifically detected by anti-FLAG and anti-HA antibodies and the levels of expression were comparable to those of the parental Gag and GagPol proteins when probed with anti-HIV-1 p24/CA and anti-HIV-1 RT antibodies. When viral particles were purified through sucrose cushions and analyzed by Western blotting, in the context of Gag-FLAG/Pol-HA, the amounts of Gag-FLAG and GagPol-HA were also comparable to those of Gag and GagPol in the parental virus

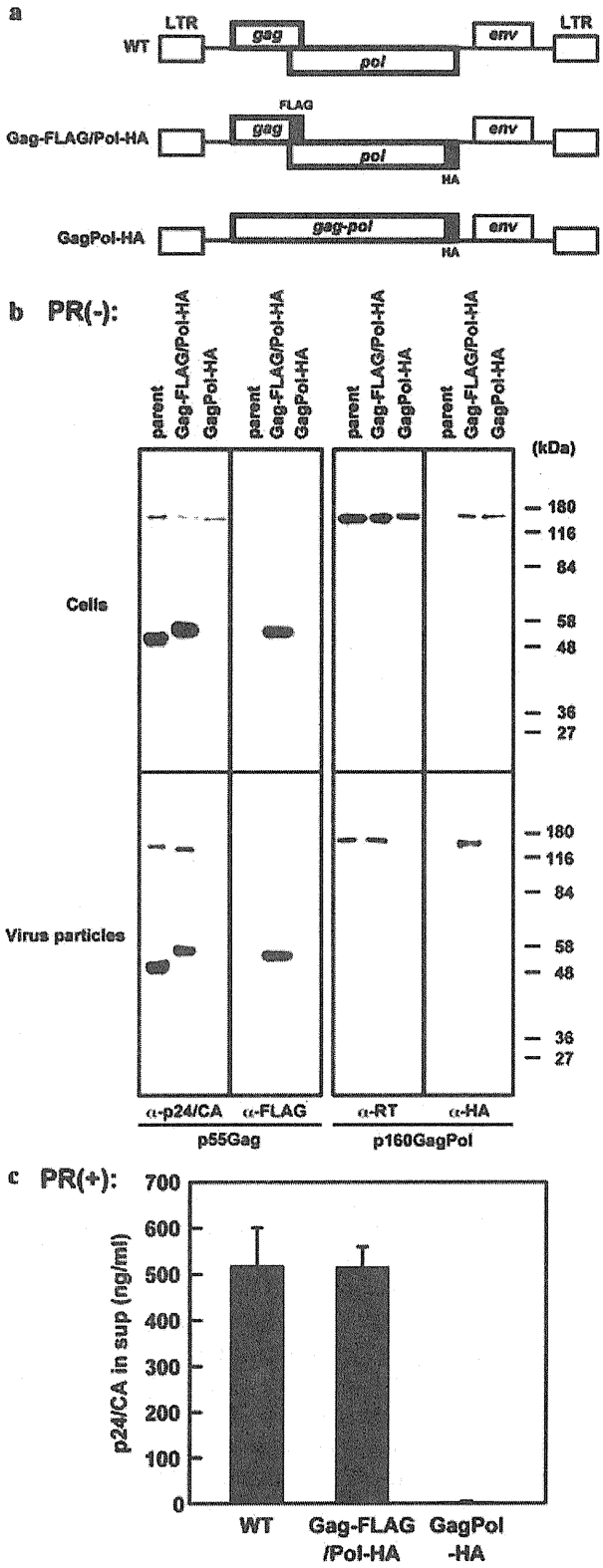

Fig. 1. Effects of epitope tagging on viral particle production. (a) Schematic representation of HIV-1 cDNA molecular clones tagged with the FLAG and HA sequences. HIV-1 molecular clone pNL43 is referred to as WT. The FLAG and HA tag sequences were inserted in-frame in the C-terminal p6 domain of the Gag protein and the C-terminus of the GagPol protein, respectively (referred to as Gag-FLAG/Pol-HA). For expression of GagPol-HA alone, the HA tag sequence was added to the C-terminus of GagPol, and the 5T sequence at the frameshift site was deleted. The same set of HIV-1 molecular clones except for an inactive form (D25N mutation) of the PR domain was similarly made. LTR, long terminal repeat. (b) Intracellular expression of Gag/GagPol and production of viral particles. HeLa cells were transfected with Gag-FLAG/Pol-HA, GagPol-HA and their parental molecular clones, all of which contain an inactive form of PR. After 48 hr, cells and viral particles were subjected to Western blotting using anti-HIV-1 p24/CA, anti-HIV-1 RT, anti-FLAG, and anti-HA antibodies. (c) Production of viral particles. HeLa cells were transfected with the WT, Gag-FLAG/Pol-HA and GagPol-HA constructs, all of which had an active form of PR. Culture media were clarified and virus particles yields (from three independent experiments) were measured by p24 antigen capture ELISA.

particles, respectively, indicating that both Gag-FLAG and GagPol-HA were incorporated into the viral particles to the same degree as occurs with authentic Gag and GagPol. Thus, the Gag-FLAG/Pol-HA construct produced a particle yield largely equivalent to that of the parental molecular clone. Particle production of the Gag-FLAG/Pol-HA construct was further examined using its molecular clone containing an active PR by HIV-1 p24/CA antigen capture ELISA, the results indicating that the Gag-FLAG/Pol-HA construct produced virus particles at a level nearly equivalent to that of WT (Fig. 1c). In contrast, expression of GagPol-HA alone did not yield virus particles, a finding which is consistent with previous studies (4, 5). These results indicate that the addition of epitope tags exerts no detrimental effects on particle production.

Gag and GagPol proteins were relocated from the cytoplasm to the plasma membrane

To gain a better understanding of the intracellular trafficking of Gag/GagPol proteins, their intracellular localization was observed by confocal microscopy at various time points (6, 12, and 24 hr post-transfection) (Fig. 2b). HeLa cells were transfected with the Gag-FLAG/Pol-HA construct, which had inactive PR, and stained with anti-FLAG and anti-HA antibodies. As shown in Figure 2a, three patterns of antigen distribution, consistent with previous studies (28, 29), were observed, namely, diffuse cytosolic distribution alone, accumulation at the plasma membrane, and punctate staining in the cytoplasm. We observed approximately 100 cells at each time point and sorted them into the three categories (Fig. 2c). As expected, Gag was diffusely distributed at 6 hr post-transfection (83.3% of Gag-positive cells) and had accumulated at the

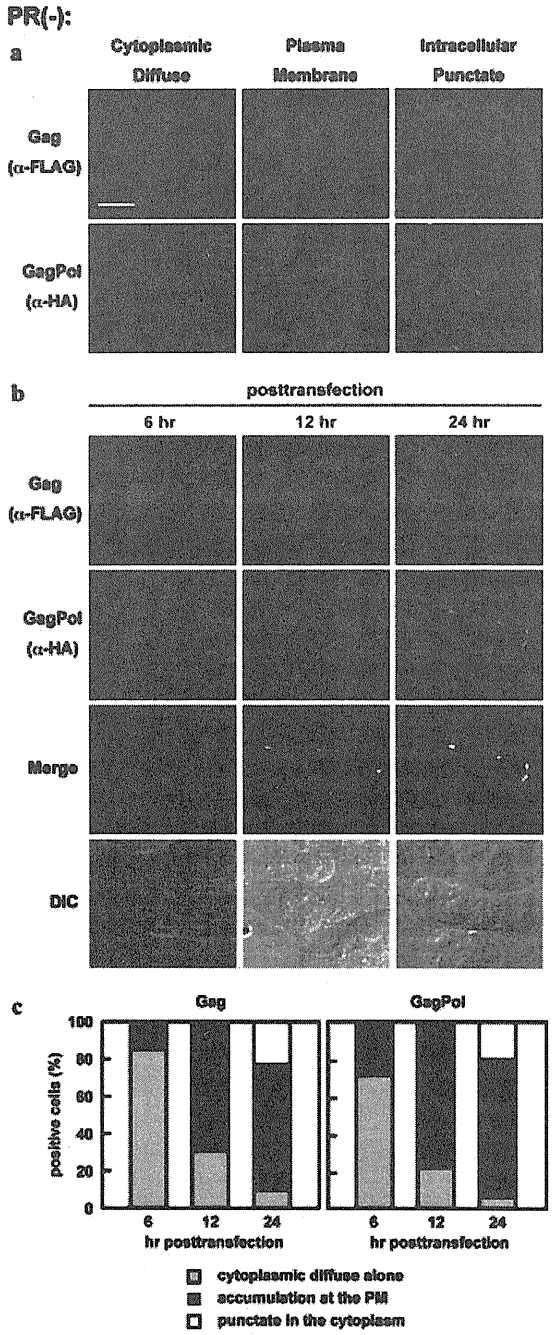

Fig. 2. Temporal study of Gag and GagPol localization. HeLa cells were transfected with the Gag-FLAG/Pol-HA construct containing an inactive form of PR. At 6, 12, and 24 hr post-transfection, cells were immunostained with anti-FLAG (for Gag) and anti-HA (for GagPol) antibodies. Nuclei were stained with TOPRO-3. All micrographs are shown at the same magnification. Bar, 10 μm. (a) Representation patterns of intracellular localization. (b) Temporal analysis of intracellular localization patterns. DIC, differential interference contrast. (c) Semiquantification of Gag and GagPol localization. Approximately 100 Gag and GagPol-positive cells were observed at each time point and the number of cells with each pattern of Gag and GagPol distribution was counted. PM, plasma membrane.

plasma membrane at 12 and 24 hr post-transfection (69.0 and 66.7% of Gag-positive cells, respectively). Punctate staining of Gag in the cytoplasm was observed frequently (24.0% of Gag-positive cells) at 24 hr post-transfection. When we observed GagPol, we found a very similar pattern of relocation: GagPol was diffusely distributed at 6 hr post-transfection (70.8% of GagPol-positive cells) and had accumulated at the plasma membrane at 12 and 24 hr post-transfection (78.9 and 74.9% of GagPol-positive cells, respectively). Overall, these data indicate that Gag and GagPol relocated from the cytoplasm to the plasma membrane. Similar observations were made when a molecular clone containing a reverse combination of tagging, Gag-HA/Pol-FLAG (data not shown) was used. Previous confocal studies have indicated that the intracellular puncta observed at late time points correspond to Gag internalized to endosomes (28).

Gag/GagPol processing occurs predominantly at the plasma membrane where Gag and GagPol co-assemble

The Pol region of GagPol contains PR that cleaves Gag and GagPol proteins and generates mature functional domains such as p17/MA, p24/CA, and RT. The profiles of Gag and GagPol processing in the Gag-FLAG/Pol-HA construct containing an active PR were examined by Western blotting using anti-RT (for p66 and p51 subunits), anti-p24/CA (for p55 precursor and mature p24/CA domain), and anti-p17/MA antibodies (for mature p17/MA domain alone) (Fig. 3a). The anti-p17/MA antibody specifically recognized the mature form of p17/MA, but not the unprocessed p55 precursor, consistent with previous studies (16). Expression of Gag/GagPol proteins was faintly detected at 6 hr post-transfection and had increased by 24 hr. Efficient processing of Gag/GagPol was observed at 24 hr post-transfection but not before that. When HeLa cells were co-stained with anti-FLAG and anti-HA antibodies and observed by confocal microscopy, Gag and GagPol were diffusely distributed at 6 hr post-transfection and had accumulated at the plasma membrane at later time points (12 and 24 hr post-transfection) (Fig. 3b), profiles which are essentially similar to those of the Gag/GagPol construct containing inactive PR (Fig. 2b). To examine intracellular sites of Gag/GagPol processing, we co-stained HeLa cells with anti-p17/MA and anti-HA antibodies. No p17/MA signals were seen at 6 hr post-transfection, by which time Gag and GagPol were diffusely distributed in the cytoplasm. At 12 and 24 hr post-transfection, punctate p17/MA signals were observed at the plasma membrane, where both Gag and GagPol had accumulated (Fig. 3b). These results suggest that Gag/GagPol processing by PR

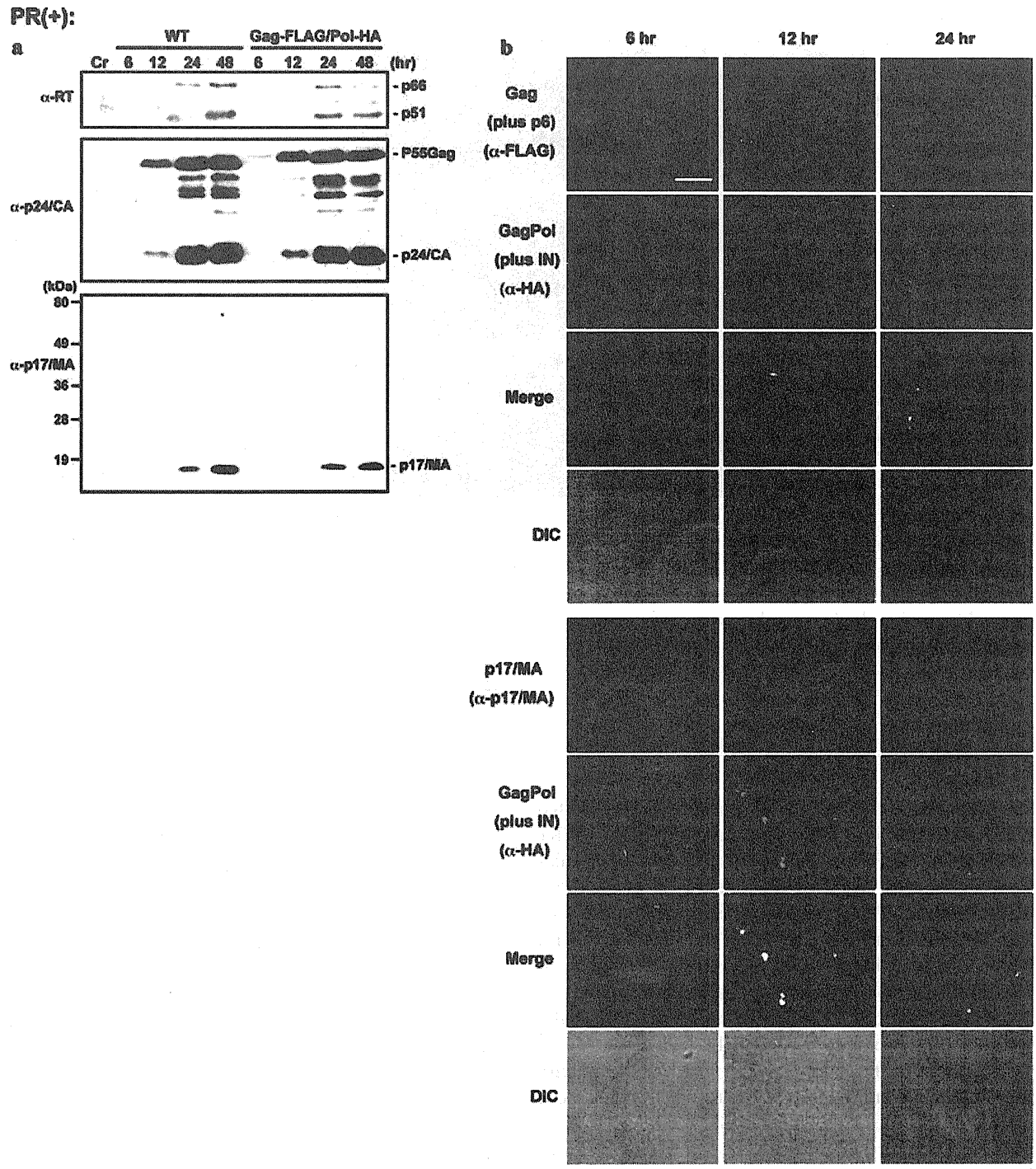

Fig. 3. Intracellular sites of Gag/GagPol processing. (a) Intracellular processing of Gag and GagPol proteins. HeLa cells were transfected with the WT and Gag-FLAG/Pol-HA constructs, both of which have an active form of PR. At 6, 12, and 24 hr post-transfection, cells were subjected to Western blotting using anti-HIV-1 p24/CA and anti-RT antibodies. Western blotting was also probed with anti-HIV-1 p17/MA antibody that specifically recognizes the mature form of p17/MA alone. (b) Intracellular localization of the mature form of p17/MA and Gag/GagPol products. HeLa cells were transfected with the Gag-FLAG/Pol-HA constructs, which have an active form of PR and were immunostained with a combination of anti-FLAG (for Gag and p6) and anti-HA (for GagPol and IN), and with a combination of anti-p17/MA (for mature MA) and anti-HA antibodies. Nuclei were stained with TOPRO-3. All micrographs are shown at the same magnification. Bar, 10 μm. DIC, differential interference contrast.

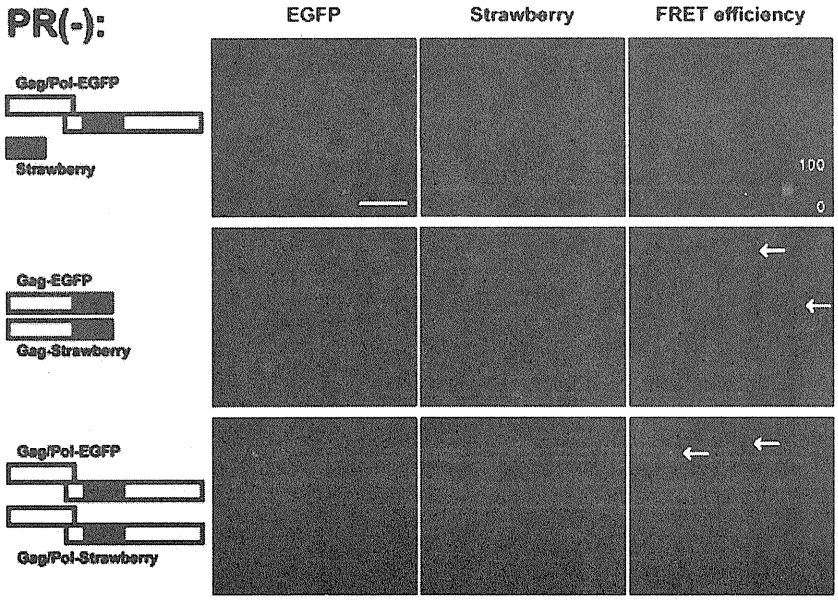

Fig. 4. Intracellular sites of GagPol dimerization. HeLa cells were cotransfected with Gag/Pol-EGFP and Gag/Pol-Strawberry constructs, both of which have an inactive form of PR. After 24 hr, cells were fixed and subjected to FRET analysis by confocal microscopy. A combination of Gag-EGFP and Gag-Strawberry constructs and a combination of Gag/Pol-EGFP construct and Strawberry (not fused to any other protein) plasmid were used as positive and negative controls, respectively. FRET efficiencies were calculated from images with three filter combinations. Arrows indicate FRET-positive puncta.

takes place at the plasma membrane during co-assembly of Gag and GagPol.

GagPol dimerization occurs predominantly at the plasma membrane

To define the sites of GagPol dimerization, we inserted EGFP and Strawberry fluorescent protein into the PR/RT junction of GagPol in the context of HIV molecular clone containing inactive PR (referred to as Gag/Pol-EGFP and Gag/Pol-Strawberry, respectively), and carried out FRET assays (Fig. 4). The Gags fused with EGFP and Strawberry at its C-termini (referred to as Gag-EGFP and Gag-Strawberry, respectively) were used as positive controls. A combination of the Gag-EGFP and Gag-Strawberry constructs exhibited robust FRET at the puncta on the plasma membrane, consistent with previous FRET analysis of Gag assembly (30). In contrast, no FRET was detected when Gag/Pol-EGFP was co-expressed with cytosolic Strawberry fluorescent protein. When FRET analysis was carried out using a combination of the Gag/Pol-EGFP and Gag/Pol-Strawberry constructs, FRET signals were only detected at the puncta on the plasma membrane (Fig. 4). To our knowledge, this is the first demonstration of GagPol-GagPol interactions. Together, these data suggest that GagPol dimerization occurs predominantly at the plasma membrane and not in the cytoplasm.

Alteration of the Gag-to-GagPol ratio has significant impacts on intracellular localization of p17/MA and viral particle production

Retroviral Gag and GagPol proteins are generated at a ratio of 10–20:1 (1). Previous studies have shown that the Gag-to-GagPol ratio has impacts on intracellular processing and viral particle production when PR is active (13). However, the localization of the processing products produced by an altered Gag-to-GagPol ratio has not been studied. We first confirmed that: (i) cotransfection of Gag-FLAG and GagPol-HA at a Gag-to-GagPol ratio of 1:0.1 produced similar amounts of virus particles to those produced by Gag-FLAG/Pol-HA; but ii) cotransfection at a Gag-to-GagPol ratio of 1:1 showed little or no particle production, although in both experiments the amount of DNA for Gag-FLAG was constant (Fig. 5a). These findings were further confirmed by electron microscopy (data not shown).

Next, we examined the intracellular distribution of the processing products by confocal microscopy (Fig. 5b) and, based on antigen distribution, the observed cells were sorted into three categories (Fig. 5c). As expected, when cells were cotransfected with Gag-FLAG and GagPol-HA at a Gag-to-GagPol DNA ratio of 1:0.1, both p17/MA and GagPol-HA (plus IN-HA) accumulated at the plasma membrane (97.8 and 79.8% of antigen-positive cells, respectively), these being similar distributions to those found in Gag-FLAG/Pol-HA-transfected cells (100 and

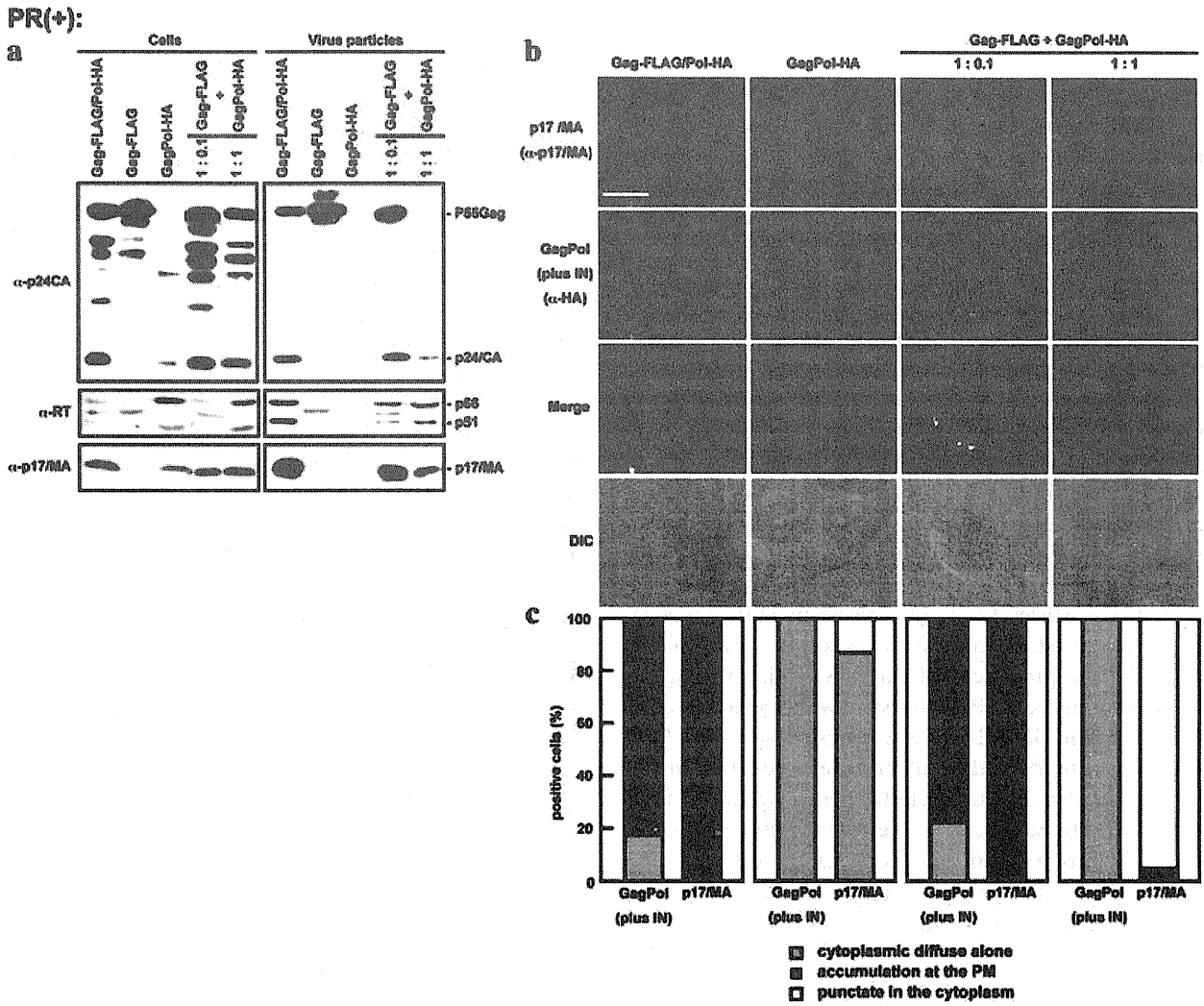

Fig. 5. Intracellular localization of mature MA and viral particle production in overexpression of GagPol containing active PR. HeLa cells were singly transfected with the Gag-FLAG/Pol-HA, GagPol-HA (both of which contain active PR), and Gag-FLAG construct, or doubly transfected with a combination of the Gag-FLAG and GagPol-HA constructs at a Gag-to-GagPol DNA ratio of 1:0.1 and 1:1. Total DNA amounts were normalized to 1.5 μg with pUC plasmid. (a) Viral particle production. Equivalent volumes of cell samples and of virus particle samples were subjected to Western blotting using anti-HIV-1 p24/CA, anti-RT, and p17/MA antibodies. (b) Intracellular localization of the mature form of p17/MA and GagPol products. At 24 hr post-transfection, cells were fixed and immunostained with anti-p17/MA (for mature MA) and anti-HA (for GagPol and IN) antibodies. Nuclei were stained with TOPRO-3. All micrographs are shown at the same magnification. Bar, 10 μm. DIC, differential interference contrast. (c) Semiquantification of localization of GagPol (plus IN), and mature MA. Approximately 50–80 antigen-positive cells were observed in each sample and the number of cells with each pattern of antigen distribution was counted. PM, plasma membrane.

84.5% of antigen-positive cells, respectively). In contrast, both antigens were diffusely distributed in the cytoplasm in cells expressing GagPol-HA alone (82.4 and 100% of antigen-positive cells, respectively). When the Gag-to-GagPol ratio was altered from 1:0.1 to 1:1, a fraction of the p17/MA population was uniformly distributed at the plasma membrane and a large population of p17/MA was observed in the cytoplasm along with punctate accumulation (95.4% of antigen-positive cells). The HA signals were also diffusely distributed in the cytoplasm (99.8% of antigen-positive cells). These patterns of antigen distribution were similarly observed at 12 hr post-transfection (data not shown). These data indicate that when PR is active, the ratio of Gag to GagPol has a significant impact on intracellular localization of their processing products.

The Gag-to-GagPol ratio has impacts on particle morphology when PR is inactive

Previous studies have suggested that when PR is inactive, the Gag-to-GagPol ratio is less critical for viral particle production, although it is still critical for virion RNA dimerization (13). We examined the impacts of the Gag-to-GagPol ratio on viral particle production using an HIV-1 molecular clone containing inactive PR. HeLa cells were cotransfected with Gag-FLAG and GagPol-HA constructs at a Gag-to-GagPol DNA ratio of 1:0.1, 1:1, and 1:10 (with a fixed amount of DNA for Gag-FLAG). Western blotting using anti-p24/CA antibody confirmed that the level of expression of Gag was constant whereas that of GagPol was increased in a DNA dose-dependent manner (Fig. 6a). As expected, the Gag-FLAG/Pol-HA construct produced viral particles containing Gag and GagPol precursors, an immature form. A number of studies have indicated that expression of the Gag region alone, or without active PR, produces an immature form of virus-like particles (2, 3, 5), consistent with our Gag-FLAG construct. In contrast, expression of GagPol-HA alone did not produce viral particles, similar to GagPol-HA containing active PR, consistent with previous studies (4, 5). When GagPol-HA was co-expressed with Gag-FLAG, we observed efficient particle production at any Gag-to-GagPol ratio that we tested here (Gag:GagPol from 1:0.1 to 1:10). Surprisingly, Western blotting using particle fractions revealed that the amounts of GagPol-HA incorporated into viral particles were increased in a DNA dose-dependent manner (Fig. 6a), indicating that a considerable number of GagPol molecules are incorporated into viral particles when its PR is inactive (compare Figs 5a and 6a). When the virus particles produced by cotransfection at a Gag-to-GagPol ratio of 1:10 were subjected to equilibrium centrifugation on sucrose gradients, they were detected at a density of 1.16–1.18 g/mL, whereas the particles obtained by the Gag-FLAG/Pol-HA construct were also sedimented (Fig. 6b). Consistent with these findings, confocal microscopy revealed that both Gag and GagPol accumulated at the plasma membrane in cells cotransfected with Gag-FLAG and GagPol-HA (Fig. 6c, d). However, when these cells were observed by electron microscopy, virus particles produced by cotransfection at a Gag-to-GagPol ratio of 1:1 and 1:10 displayed aberrant morphology: not hollow but encasing electron-dense amorphous materials. In contrast, cotransfection at a ratio of 1:0.1 produced doughnut-like particles, characteristic of the immature form (Fig. 6e). Together, these data suggest that the Gag-to-GagPol ratio has substantial impacts on particle morphology even when PR is inactive.

DISCUSSION

Gag processing and GagPol dimerization at sites on the plasma membrane where Gag and GagPol are assembled

It is generally accepted that retroviral GagPol protein is incorporated into virus particles through co-assembly with Gag protein, since GagPol protein alone does not produce viral particles but it is incorporated into viral particles when co-expressed with Gag (4, 5). We confirmed these observations and further found that both Gag and GagPol are relocated from the cytoplasm to the plasma membrane and subsequently accumulate at certain sites on the plasma membrane (Figs 2, 3). These sites are most likely to be lipid raft microdomains because they have been suggested to be sites of virus particle assembly for many viruses including HIV (31–34). In this study, we used anti-HIV-1 p17/MA monoclonal antibody that only recognizes mature cleaved MA and demonstrated that Gag processing, at least cleavage of the MA/CA junction, occurred predominantly during assembly at the plasma membrane. Previous studies of *in vitro* processing have described the order of Gag processing: Gag protein is initially cleaved at the p2/NC junction, followed by the MA/CA junction, and finally at the CA/p2 junction (p2/NC > NC/p6 ≥ MA/CA > CA/p2) (35, 36). Although these data raise the possibility that initial cleavage of the p2/NC junction might start during membrane trafficking, we suggest this possibility is unlikely because FRET signals with GagPol dimerization were predominantly observed at the plasma membrane (Fig. 4) even when the constructs contained an active PR (data not shown).

We employed confocal microscopy-based FRET assays to detect the sites of GagPol dimerization and found that it essentially occurs at sites of the plasma membrane where Gag and GagPol have accumulated (Fig. 4). Similarly, many studies have indicated that HIV Gag is multimerized after membrane targeting, suggesting that Gag oligomers formed in the cytosol before membrane targeting are possibly dead-end products (37, 38). It is tempting to speculate that in expression at a normal Gag-to-GagPol ratio, efficient dimerization of Gag-Pol might be suppressed during plasma membrane trafficking, resulting in no PR activity. However, because the FRET system used here was based on EGFP-to-Strawberry (green-to-red) FRET, which is specific with lower background but less sensitive than cyan fluorescent protein-to-yellow fluorescent protein FRET, we cannot rule out that a fraction of GagPol dimers below our detection limitation might have been present in the cytoplasm.

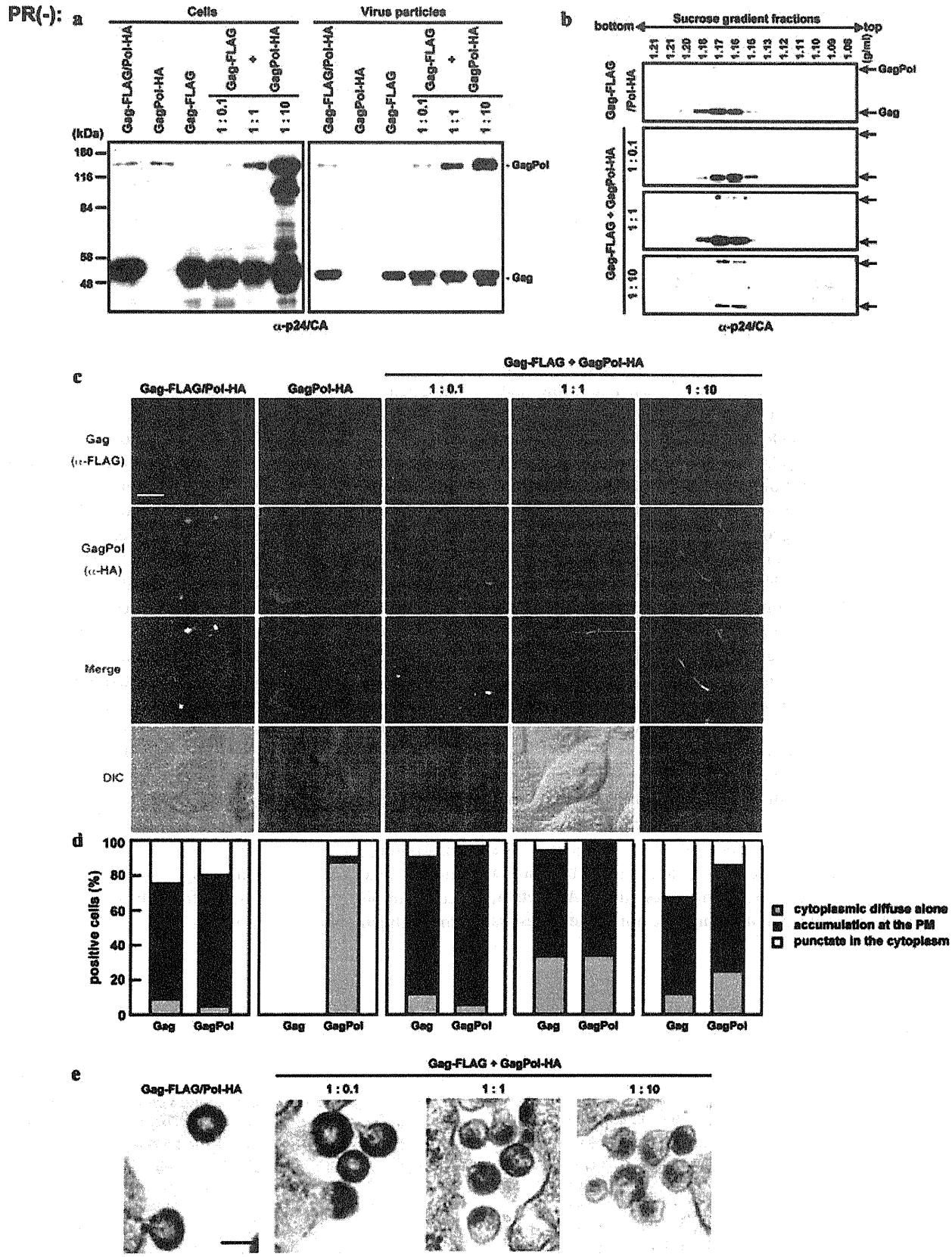

Premature processing by overexpression of GagPol

Previous studies have shown that overexpression of GagPol alone results in absence of particle production (10, 12) and that coexpression of Gag and GagPol at a nearly equimolar ratio severely impairs particle production (13). In this study, we observed the sites of Gag processing under these overexpression conditions. Our confocal data revealed that cleaved p17/MA was diffusely distributed in the cytoplasm when GagPol was expressed alone, suggesting that Gag processing might have occurred before membrane targeting of GagPol (Fig. 5). Interestingly, the equimolar cotransfection of Gag and GagPol constructs exhibited unique distribution patterns of p17/MA: uniform distribution at the plasma membrane and punctate accumulation in the cytoplasm (Fig. 5). The former pattern may result from Gag processing after plasma membrane targeting but before Gag assembly, whereas the latter may represent cytoplasmic processing and/or retargeting to cellular membranous compartments, although these are not proven in this study. Previous studies have shown that cleavage of GagPol occurs even when GagPol lacks the myristoylation signal (5, 12), suggesting there is no relationship between N-terminal myristoylation and processing. Rather, it is conceivable that if the amount of Gag is higher than that of GagPol, GagPol preferentially interacts with Gag and is transported to the plasma membrane (by virtue of the membrane targeting signals of Gag), where it accumulates and forms a homodimer, resulting in PR activation and subsequent Gag/GagPol processing at the plasma membrane. In contrast, when the amount of GagPol is higher than that of Gag, GagPol may preferentially interact with GagPol and form a homodimer in the cytoplasm. This GagPol dimerization would result in aberrant Gag/GagPol processing in the cytoplasm. The resultant processing products would not reach the plasma membrane or participate in virion assembly. Altogether, overexpression of GagPol beyond the normal level results in aberrant distribution of mature cleaved p17/MA, which does not contribute to efficient particle production. Thus, the Gag-to-GagPol ratio has significant impacts on particle assembly when PR is active.

Incorporation of GagPol precursors into virus particles

The incorporation of GagPol precursors containing inactive PR into virus particles has been studied by expression of the *gag-pol* region containing an inactive PR domain and by cotransfection experiments with Gag and GagPol constructs containing inactive PR (4, 5). One study has suggested that nearly equimolar cotransfection of Gag and GagPol constructs produces virus particles as efficiently as expression of the Gag construct alone (5). However in another study, especially when the GagPol construct was cotransfected with the HIV molecular clone, virus particle production was slightly impaired, although the impacts were much less than those observed when PR was active (13). To understand to what extent GagPol molecules can be incorporated into virus particles, we altered the Gag-to-GagPol ratio from 1:0.1 to 1:10 and carried out cotransfection experiments. Surprisingly, we found that the amounts of GagPol incorporated into viral particles increased in a DNA dose-dependent manner (Fig. 6a). These data suggest that the incorporation limitation of GagPol molecules into virus particles is not strictly regulated when its PR is inactive. However, our electron microscopy data indicated that particle morphology became aberrant when the Gag-to-GagPol ratio was altered from 1:0.1 to 1:1 or 1:10 (Fig. 6e), implying that the Gag-to-GagPol ratio has substantial impacts on particle morphology even when PR is inactive. Careful observation of the aberrance in particle morphology, namely amorphous materials encased in particles, suggested that Gag and GagPol might not properly co-assemble or easily dissociate from the envelope membrane during/after particle budding (Fig. 7). We speculate

Fig. 6. Intracellular localization of Gag/GagPol precursors and viral particle production in overexpression of GagPol containing inactive PR. HeLa cells were singly transfected with the Gag-FLAG/Pol-HA, GagPol-HA, and Gag-FLAG construct, or doubly transfected with a combination of the Gag-FLAG and GagPol-HA constructs at a Gag-to-GagPol DNA ratio of 1:0.1, 1:1, and 1:10. Total DNA amounts were normalized to 1.5 μg with pUC plasmid. (a) Virus particle production. Equivalent volumes of cell samples and virus particle samples were subjected to Western blotting using anti-HIV-1 p24/CA antibody. (b) Equilibrium gradient centrifugation of virus particles. Produced particles were applied onto 20–60% (w/v) sucrose gradients and centrifuged at 4°C at 120,000 × *g* overnight. Gradient fractions were analyzed by Western blotting using anti-p24/CA antibody. (c) Intracellular localization of Gag and GagPol proteins. At 24 hr post-transfection, cells were fixed and immunostained with anti-FLAG (for Gag) and anti-HA (for GagPol) antibodies. Nuclei were stained with TOPRO-3. All micrographs are shown at the same magnification. Bar, 10 μm. DIC, differential interference contrast. (d) Semiquantification of Gag and GagPol localization. Approximately 100 antigen-positive cells were observed in each sample and the number of cells with each pattern of Gag and GagPol distribution was counted. PM, plasma membrane. (e) Electron microscopy. All micrographs are shown at the same magnification. Bar, 100 nm.

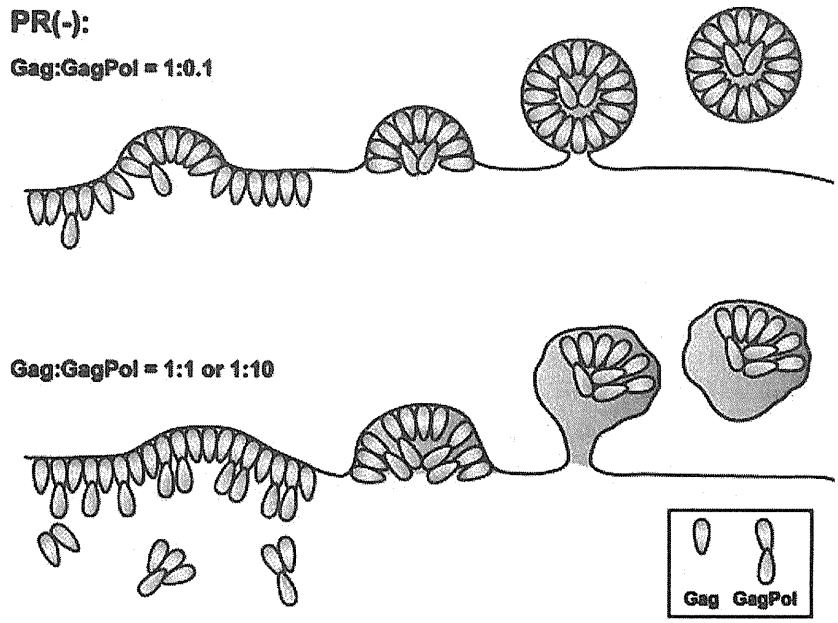

Fig. 7. A model for viral particle production in overexpression of GagPol containing an inactive PR. When the Gag-to-GagPol ratio is 1:0.1, both molecules target to the plasma membrane and assemble into spherical virus particles that exhibit doughnut-like morphology, characteristic of the immature form. When the Gag-to-GagPol ratio is 1:1 or 1:10, both molecules target to the plasma membrane but, because GagPol is considerably larger and less competent at membrane association than Gag, budding particles may exhibit aberrant assembly morphology with irregular membrane curvature. Budding particles may accommodate eccentric cores, possibly representing aggregation of Gag/GagPol molecules after dissociation from the particle membrane.

that GagPol may have intrinsically negative effects on its membrane binding and/or assembly.

ACKNOWLEDGMENTS

We thank Y. Tsunetsugu-Yokota for supply of anti-HIV-1 p24 mouse antibody. This work was supported by an AIDS grant from the Ministry of Health, Labor, and Welfare of Japan, by a Grant-in-Aid for Scientific Research from the Japan Society for the Promotion of Science, in part by Grants-in-Aid for Specially Promoted Research and for Scientific Research, by Exploratory Research for Advanced Technology (Japan Science and Technology Agency), and by the National Institute of Allergy and Infectious Diseases Public Health Service research grants, USA.

REFERENCES

1. Jacks T., Power M.D., Masiarz F.R., Luciw P.A., Barr P.J., Varmus H.E. (1988) Characterization of ribosomal frameshifting in HIV-1 gag-pol expression. *Nature* **331:** 280–3.
2. Gheysen D., Jacobs E., de Foresta F., Thiriart C., Francotte M., Thines D., de Wilde M. (1989) Assembly and release of HIV-1 precursor Pr55gag virus-like particles from recombinant baculovirus-infected insect cells. *Cell* **59:** 103–12.
3. Morikawa Y. (2001) HIV capsid assembly. *Curr HIV Res* **1:** 1–14
4. Park J., Morrow C.D. (1992) The nonmyristylated Pr160gag-pol polyprotein of human immunodeficiency virus type 1 interacts with Pr55gag and is incorporated into virus-like particles. *J Virol* **66:** 6304–13.
5. Smith A.J., Srinivasakumar N., Hammarskjold M.L., Rekosh D. (1993) Requirements for incorporation of Pr160*gag-pol* from human immunodeficiency virus type 1 into virus-like particles. *J Virol* **67:** 2266–75.
6. Mervis R.J., Ahmad N., Lillehoj E.P., Raum M.G., Salazar F.H., Chan H.W., Venkatesan S. (1988) The *gag* gene products of human immunodeficiency virus type 1: alignment within the *gag* open reading frame, identification of posttranslational modifications, and evidence for alternative *gag* precursors. *J Virol* **62:** 3993–4002.
7. Gottlinger H.G., Sodroski J.G., Haseltine W.A. (1989) Role of capsid precursor processing and myristoylation in morphogenesis and infectivity of human immunodeficiency virus type 1. *Proc Natl Acad Sci USA* **86:** 5781–5.
8. Rose J.R., Babe L.M., Craik, C.S. (1995) Defining the level of human immunodeficiency virus type 1 (HIV-1) protease activity required for HIV-1 particle maturation and infectivity. *J Virol* **69:** 2751–8.
9. Kaplan A.H., Manchester M., Swanstrom R. (1994) The activity of the protease of human immunodeficiency virus type 1 is initiated at the membrane of infected cells before the release of viral proteins and is required for release to occur with maximum efficiency. *J Virol* **68:** 6782–6.
10. Karacostas V., Wolffe E.J., Nagashima K., Gonda M.A., Moss B. (1993) Overexpression of the HIV-1 *gag-pol* polyprotein results in intracellular activation of HIV-1 protease and inhibition of assembly and budding of virus-like particles. *Virology* **193:** 661–71.
11. Krausslich H.G. (1991) Human immunodeficiency virus proteinase dimer as component of the viral polyprotein prevents particle assembly and viral infectivity. *Proc Natl Acad Sci USA* **88:** 3213–17.
12. Park J., Morrow C.D. (1991) Overexpression of the gag-pol precursor from human immunodeficiency virus type 1 proviral genomes results in efficient proteolytic processing in the absence of virion production. *J Virol* **65:** 5111–7.
13. Shehu-Xhilaga M., Crowe S.M., Mak J. (2001) Maintenance of the Gag/Gag-Pol ratio is important for human immunodeficiency virus type 1 RNA dimerization and viral infectivity. *J Virol* **75:** 1834–41.
14. Louis J.M., Clore G.M., Gronenborn A.M. (1999) Autoprocessing of HIV-1 protease is tightly coupled to protein folding. *Nat Struct Biol* **6:** 868–75.

15. Tang C., Louis J.M., Aniana A., Suh J-Y., Clore G.M. (2008) Visualizing transient events in amino-terminal autoprocessing of HIV-1 protease. *Nature* **455:** 693–6.
16. Suyama M., Daikoku E., Goto T., Sano K., Morikawa Y. (2009) Reactivation from latency displays HIV particle budding at plasma membrane, accompanying CD44 upregulation and recruitment. *Retrovirology* **6:** 63.
17. Adachi A., Gendelman H.E., Koenig S., Folks T., Willey R., Rabson A., Martin M.A. (1986) Production of acquired immunodeficiency syndrome-associated retrovirus in human and nonhuman cells transfected with an infectious molecular clone. *J Virol* **59:** 284–91.
18. Huang M., Orenstein J.M., Martin M.A., Freed E.O. (1995) p6Gag is required for particle production from full-length human immunodeficiency virus type 1 molecular clones expressing protease. *J Virol* **69:** 6810–18.
19. Tsunetsugu-Yokota Y., Ishige M., Murakami M. (2007) Oral attenuated *Salmonella enterica* serovar Typhimurium vaccine expressing codon-optimized HIV type 1 Gag enhanced intestinal immunity in mice. *AIDS Res Hum Retroviruses* **23:** 278–286.
20. Feige J.N., Sage D., Wahli W., Desvergne B., Gelman L. (2005) PixFRET, an ImageJ plug-in for FRET calculation that can accommodate variations in spectral bleed-throughs. *Microsc Res Tech* **68:** 51–8.
21. Demirov D.G., Ono A., Orenstein J.M., Freed E.O. (2002) Overexpression of the N-terminal domain of TSG101 inhibits HIV-1 budding by blocking late domain function. *Proc Natl Acad Sci USA* **99:** 955–60.
22. Garrus J.E., von Schwedler U.K., Pornillos O.W., Morham S.G., Zavitz K.H., Wang H.E., Wettstein D.A., Stray K.M., Cote M., Rich R.L., Myszka D.G., Sundquist W.I. (2001) Tsg101 and the vacuolar protein sorting pathway are essential for HIV-1 budding. *Cell* **107:** 55–65.
23. Strack B., Calistri A., Craig S., Popova E., Gottlinger H.G. (2003) AIP1/ALIX is a binding partner for HIV-1 p6 and EIAV p9 functioning in virus budding. *Cell* **114:** 689–99.
24. VerPlank L., Bouamr F., LaGrassa T.J., Agresta B., Kikonyogo A., Leis J., Carter C.A. (2001) Tsg101, a homologue of ubiquitin-conjugating (E2) enzymes, binds the L domain in HIV type 1 Pr55(Gag). *Proc Natl Acad Sci USA* **98:** 7724–9.
25. von Schwedler U.K., Stuchell M., Muller B., Ward D.M., Chung H.Y., Morita E., Wang H.E., Davis T., He G.P., Cimbora D.M., Scott A., Krausslich H.G., Kaplan J., Morham S.G., Sundquist W.I. (2003) The protein network of HIV budding. *Cell* **114:** 701–13.
26. Kondo E., Gottlinger H.G. (1996) A conserved LXXLF sequence is the major determinant in p6gag required for the incorporation of human immunodeficiency virus type 1 Vpr. *J Virol* **70:** 159–64.
27. Lu Y.L., Bennett R.P., Wills J.W., Gorelick R., Ratner L. (1995) A leucine triplet repeat sequence (LXX)4 in p6gag is important for Vpr incorporation into human immunodeficiency virus type 1 particles. *J Virol* **69:** 6873–9.
28. Jouvenet N., Neil S.J., Bess C., Johnson M.C., Virgen C.A., Simon S.M., Bieniasz P.D. (2006) Plasma membrane is the site of productive HIV-1 particle assembly. *PLoS Biol* **4:** e435.
29. Kawada S., Goto T., Haraguchi H., Ono A., Morikawa Y. (2008) Dominant negative inhibition of human immunodeficiency virus particle production by the nonmyristoylated form of gag. *J Virol* **82:** 4384–99.
30. Hogue I.B., Hoppe A., Ono A. (2009) Quantitative fluorescence resonance energy transfer microscopy analysis of the human immunodeficiency virus type 1 Gag-Gag interaction: relative contributions of the CA and NC domains and membrane binding. *J Virol* **83:** 7322–36.
31. Holm K., Weclewicz K., Hewson R., Suomalainen M. (2003) Human immunodeficiency virus type 1 assembly and lipid rafts: Pr55(gag) associates with membrane domains that are largely resistant to Brij98 but sensitive to Triton X-100. *J Virol* **77:** 4805–17.
32. Lindwasser O.W., Resh M.D. (2001) Multimerization of human immunodeficiency virus type 1 Gag promotes its localization to barges, raft-like membrane microdomains. *J Virol* **75:** 7913–24.
33. Nguyen D.H., Hildreth J.E. (2000) Evidence for budding of human immunodeficiency virus type 1 selectively from glycolipid-enriched membrane lipid rafts. *J Virol* **74:** 3264–72.
34. Ono A., Freed E.O. (2001) Plasma membrane rafts play a critical role in HIV-1 assembly and release. *Proc Natl Acad Sci USA* **98:** 13,925–30.
35. Pettit S.C., Moody M.D., Wehbie R.S., Kaplan A.H., Nantermet P.V., Klein C.A., Swanstrom R. (1994) The p2 domain of human immunodeficiency virus type 1 Gag regulates sequential proteolytic processing and is required to produce fully infectious virions. *J Virol* **68:** 8017–27.
36. Tritch R.J., Cheng Y.E., Yin F.H., Erickson-Viitanen S. (1991) Mutagenesis of protease cleavage sites in the human immunodeficiency virus type 1 *gag* polyprotein. *J Virol* **65:** 922–30.
37. Li H., Jun D., Ding L., Spearman P. (2007) Myristoylation is required for human immunodeficiency virus type 1 Gag-Gag multimerization in mammalian cells. *J Virol* **81:** 12,899–910
38. Tritel M., Resh, M.D. (2000) Kinetic analysis of human immunodeficiency virus type 1 assembly reveals the presence of sequential intermediates. *J Virol* **74:** 5845–55.

OPEN ACCESS Freely available online

PLoS one

Allosteric Regulation of HIV-1 Reverse Transcriptase by ATP for Nucleotide Selection

Masaru Yokoyama*, Hiromi Mori, Hironori Sato

Pathogen Genomics Center, National Institute of Infectious Diseases, Musashi Murayama-shi, Tokyo, Japan

Abstract

Background: Human immunodeficiency virus type 1 reverse transcriptase (HIV-1 RT) is a DNA polymerase that converts viral RNA genomes into proviral DNAs. How HIV-1 RT regulates nucleotide selectivity is a central issue for genetics and the nucleoside analog RT inhibitor (NRTI) resistance of HIV-1.

Methodology/Principal Findings: Here we show that an ATP molecule at physiological concentrations acts as an allosteric regulator of HIV-1 RT to decrease the K_m value of the substrate, decrease the k_{cat} value, and increase the K_i value of NRTIs for RT. Computer-assisted structural analyses and mutagenesis studies suggested the positions of the ATP molecule and NRTI-resistance mutations during a catalytic reaction, which immediately predict possible influences on nucleotide insertion into the catalytic site, the DNA polymerization, and the excision reaction.

Conclusions/Significance: These data imply that the ATP molecule and NRTI mutations can modulate nucleotide selectivity by altering the fidelity of the geometric selection of nucleotides and the probability of an excision reaction.

Citation: Yokoyama M, Mori H, Sato H (2010) Allosteric Regulation of HIV-1 Reverse Transcriptase by ATP for Nucleotide Selection. PLoS ONE 5(1): e8867. doi:10.1371/journal.pone.0008867

Editor: Jean-Pierre Vartanian, Institut Pasteur, France

Received October 28, 2009; **Accepted** January 5, 2010; **Published** January 25, 2010

Funding: This work was supported by a grant from the Ministry of Health, Labor and Welfare, Japan. The funders had no role in study design, data collection and analysis, decision to publish, or preparation of the manuscript.

Competing Interests: The authors have declared that no competing interests exist.

* E-mail: yokoyama@nih.go.jp

Introduction

Human immunodeficiency virus type 1 reverse transcriptase (HIV-1 RT) is an RNA-dependent DNA polymerase that converts single-stranded viral RNA genomes into double-stranded proviral DNAs after HIV-1 entry into the cells. Active HIV-1 RT is composed of two related chains, termed p51 and p66 [1]. The p66 chain has a catalytic site for DNA polymerization: the fingers, palm, and thumb subdomains form a cavity for the binding of the template, primer, two divalent cations, and dNTPs for DNA synthesis [1], as seen in other DNA polymerases. Although HIV-1 RT exhibits no exonucleolytic proofreading activity, it still retains a relatively high level of fidelity of DNA synthesis, i.e., about $2.5–6\times10^{-4}$ base substitutions per site [2,3]. Increasing evidence suggests that the high fidelity of DNA synthesis achieved by DNA polymerases—i.e., the discrimination of the correct and incorrect nucleotides for polymerization—is primarily due to the geometric selection of nucleotides during nucleotide insertion into the catalytic site [4,5,6].

An ATP molecule is a multifunctional nucleotide that exists at a concentration of ~3.2 mM in the cells [7]. Many studies have suggested that the ATP molecule is a cellular factor involved in the drug resistance of HIV-1. Nucleoside analog RT inhibitors (NRTIs) act as chain terminators blocking DNA synthesis, since they lack the 3′-OH group required for the phosphodiester bond formation, whereas NRTI-resistant RT catalyzes dinucleoside polyphosphate synthesis in the presence of millimolar concentrations of NTP [8]. Thus, the ATP molecule at physiological concentrations *in vitro* serves as an effective pyrophosphate donor to the excision reaction of the RT to remove the chain terminating NRTIs [8,9,10]. A previous crystal structure study identified a binding site of ATP in the catalytic cavity of p66 when the RT was free from the template and primer [11]. Although ATP-mediated excision provides a plausible mechanism for the NRTI resistance of HIV-1, some NRTI-resistance mutations are located distantly from the excision site. Therefore, their roles in NRTI resistance are not fully understood [12].

Enzyme activity is often modulated by an allosteric effector, a small natural compound that binds to the enzyme at a site distinct from the substrate-binding site. In this study, we show by kinetic, structural, and mutagenesis studies that the ATP molecule can act as an allosteric effector of HIV-1 RT to modulate nucleotide selectivity and DNA polymerization. We also show probable three-dimensional (3-D) positions of the bound ATP molecule and NRTI-resistance mutations during a catalytic cycle. The obtained data suggest that the ATP molecule and NRTI mutations can cooperatively modulate physicochemical properties of the p66 catalytic cavity to alter the fidelity of the geometric selection of nucleotides and the probability of an excision reaction.

Results

Effects of ATP on HIV-1 RT Reaction Kinetics

First, we analyzed the effects of ATP on HIV-1 RT reaction kinetics. We began by collecting basic information on the steady-state kinetics of DNA polymerization in the absence of the ATP molecule. We used two HIV-1 RTs for the present study: the

NRTI-sensitive RT (93JP-NH1) and multi-NRTI-resistant RT (ERT-mt6) [13]. The ERT-mt6 RT has an 11-amino-acid insertion in the β3-β4 loops of the p66 fingers subdomain and four substitutions–M41L, T69I, L210W, and T215Y–in the polypeptide backbone of 93JP-NH1 [13]. These mutations confer higher levels of resistance of the 93JP-NH1 virus against AZT, d4T, β-L-2′,3′-dideoxy-3-thiacytidine, 2′,3′-dideoxyinosine, and 2′,3′-dideoxycytidine than other mutants in the polypeptide backbone of 93JP-NH1 [13]. Therefore, we used ERT-mt6 RT, which clearly showed that NRTI-resistance mutations enhance the effect of ATP on enzyme kinetics in NRTI-sensitive RT.

The initial velocities of dTTP incorporation into poly (rA)·p(dT)$_{12-18}$ were measured using purified p51/p66 RT heterodimers of the 93JP-NH1 and ERT-mt6 RTs (Figure S1A). In both RTs, the dTTP incorporation followed Michaelis-Menten kinetics (Figure S1B). The K_m values for the 93JP-NH1 and ERT-mt6 RTs were 4.0±0.1 and 13.8±0.5 μM, respectively, suggesting that the dTTP has a higher K_m value for ERT-mt6 RT. The k_{cat} values for 93JP-NH1 and ERT-mt6 RTs were 1.04±0.01 and 0.49±0.01s^{-1}, respectively, suggesting that ERT-mt6 RT has a nucleotide addition reaction with a slower turnover rate.

We then used the two RTs to examine whether or not the ATP molecule influences the DNA polymerization kinetics by measuring the initial velocity of dTTP incorporation into poly (rA)·p(dT)$_{12-18}$ in the presence of 0, 1, 2, 3, and 4 mM of ATP. The velocity is decreased in both RTs in association with an increase in ATP concentration, indicating that the ATP molecule inhibits the overall catalytic reaction by HIV-1 RT (Figure 1A). Lineweaver-Burk double-reciprocal plots showed that, in both RTs, the straight lines at the different ATP concentrations have different x- and y-intercepts, and that the line slope increases with increasing ATP concentration (Figure 1B). The data suggest that the ATP-mediated inhibition of dTTP incorporation is a mixed noncompetitive inhibition.

We further examined whether or not the ATP molecule can influence the K_m of substrate and k_{cat} values in the enzyme reaction. The substrate-velocity data in Figure 1A were fit to Equations 1 and 2 (see Materials and Methods), and the average K_m and k_{cat} values in the presence of 0, 1, 2, 3, and 4 mM of ATP were obtained with six independent experiments. Notably, both K_m and k_{cat} values for the 93JP-NH1 and ERT-mt6 RTs monotonically decreased with increasing ATP concentration (Figure 1C).

We also examined the K_i values of ATP to the two RTs. On the basis of information on the RT catalytic cycle [14], we assumed two structures of RT for ATP binding: the RT-template-primer complex (RT complex 1) and the RT-template-primer-dTTP complex (RT complex 2). Using Equations 3 and 4 (see Materials and Methods), we calculated K_i^{ATP} and $K_i'^{ATP}$ values of ATP to the RT complexes 1 and 2, respectively. The K_i^{ATP} values were 2.9±1.3 and 2.8±1.3 mM for the 93JP-NH1 and ERT-mt6 RTs, respectively, suggesting that the ATP molecule binds with the equivalent K_i^{ATP} value to complex 1 of the two RTs. The $K_i'^{ATP}$ values were 1.2±0.5 and 1.1±0.4 mM for the 93JP-NH1 and ERT-mt6 RTs, respectively, suggesting that the ATP molecule also binds with the equivalent $K_i'^{ATP}$ value to complex 2 of these RTs. These results are consistent with the finding that AZT resistance mutations cause no difference in ATP binding [15,16]. Finally, the K_i^{ATP} value was larger than the $K_i'^{ATP}$ value in both RTs, suggesting that ATP binds with higher affinity to the dTTP-bound RT than to the substrate-free RT.

ATP's Effects on NRTI Action

Next, we examined whether or not the ATP molecule influences the action of NRTI on the two RTs. In the absence of the ATP molecule, nanomole orders of AZTTP effectively inhibited dTTP incorporation by both RTs (Figure 2A, top), suggesting that, in the absence of the ATP molecule, the level of inhibition of DNA polymerization by AZTTP is equivalent between the two RTs. In the presence of 1 mM ATP, the inhibition was more moderate with the ERT-mt6 RT than with the 93JP-NH1 RT, and the difference in the inhibition curve became much greater in the presence of 5 mM ATP (Figure 2A, middle and bottom). These data suggest that the ATP molecule and NRTI mutations cooperatively reduce the NRTI sensitivity of HIV-1 RT *in vitro*.

We next examined whether or not the above ATP effects on NRTI resistance were specific to the ATP molecule by measuring the IC$_{50}$ of AZTTP in the presence of 5 mM UTP, CTP, GTP, NaPO$_4$, dATP, ADP, cAMP, and AMP-PNP (Figure 2B). While many of the compounds tested increased the IC$_{50}$ of AZTTP, the magnitude of the fold increase was consistently greater with ERT-mt6 RT than 93JP-NH1 RT. The ATP molecule was most effective at increasing the IC$_{50}$, yielding an approximately 350-fold increase with the ERT-mt6 RT. The ATP, dATP, and GTP molecules, which have a purine ring, had greater effects on the IC$_{50}$ increase than the UTP and CTP molecules, which have a pyrimidine ring. NaPO$_4$ and cAMP had little effect on the IC$_{50}$ in either RT. Notably, AMP-PNP, a non-hydrolyzed analogue of the ATP molecule, also increased the IC$_{50}$ of AZTTP by approximately 150-fold with the ERT-mt6 RT. These data suggest that nucleotides similar in size to the ATP molecule can assist in the development of NRTI resistance.

We further examined whether or not the ATP molecule influences the K_i values of AZTTP and d4TTP to the two RTs in the enzyme reaction. Based on the kinetics data for ATP in Figure 1, the kinetics data for AZTTP in Figure S2, the reported kinetics data for AZTTP inhibition [17,18], and a crystal structure study of the ATP-RT complex [11], a simplified kinetics model in which ATP functions as a mixed noncompetitive inhibitor and nucleoside analogs function as competitive inhibitors was hypothesized (Figure 2C). We measured the initial velocities of dTTP incorporation by HIV-1 RTs at various ATP concentrations and various AZTTP or d4TTP concentrations, and calculated the K_i values of these compounds for the 93JP-NH1 and ERT-mt6 RTs using Equations 5 and 6 (see Materials and Methods). Notably, the ATP molecule induced increases in the K_i^{NRTI} value in a dose-dependent manner. The magnitudes of the increases were much greater with ERT-mt6 RT, reaching about 30-fold for the K_i^{AZTTP} value and 8.5-fold for the K_i^{d4TTP} value at 3 mM of ATP compared to those without the ATP molecule (Figure 2D). The magnitude of changes in K_i^{NRTI} values was much smaller with 93JP-NH1 RT, which yielded about 6.8- and 0.6-fold increases in K_i^{AZTTP} and K_i^{d4TTP} values, respectively, at 3 mM of ATP compared to those without the ATP molecule. These data suggest that physiological concentrations of ATP [7] potently increase the K_i value of NRTI when RT has NRTI-resistance mutations.

Structural Study on ATP Action

A previous study identified a binding site of the ATP molecule in the p66 when the RT was free from the template and primer [11]. To address the binding site of the ATP molecule in RT during DNA synthesis, we conducted a computer-assisted structural analysis. Using the homology modeling method [19], we first constructed 3-D models of 93JP-NH1 and ERT-mt6 RTs at various catalytic stages defined by biochemical and crystallographic data [14,20,21] (Figure 3). In the DNA polymerization processes, each single nucleotide addition cycle was divided into four steps, termed the post-translocation, fingers-open ternary,

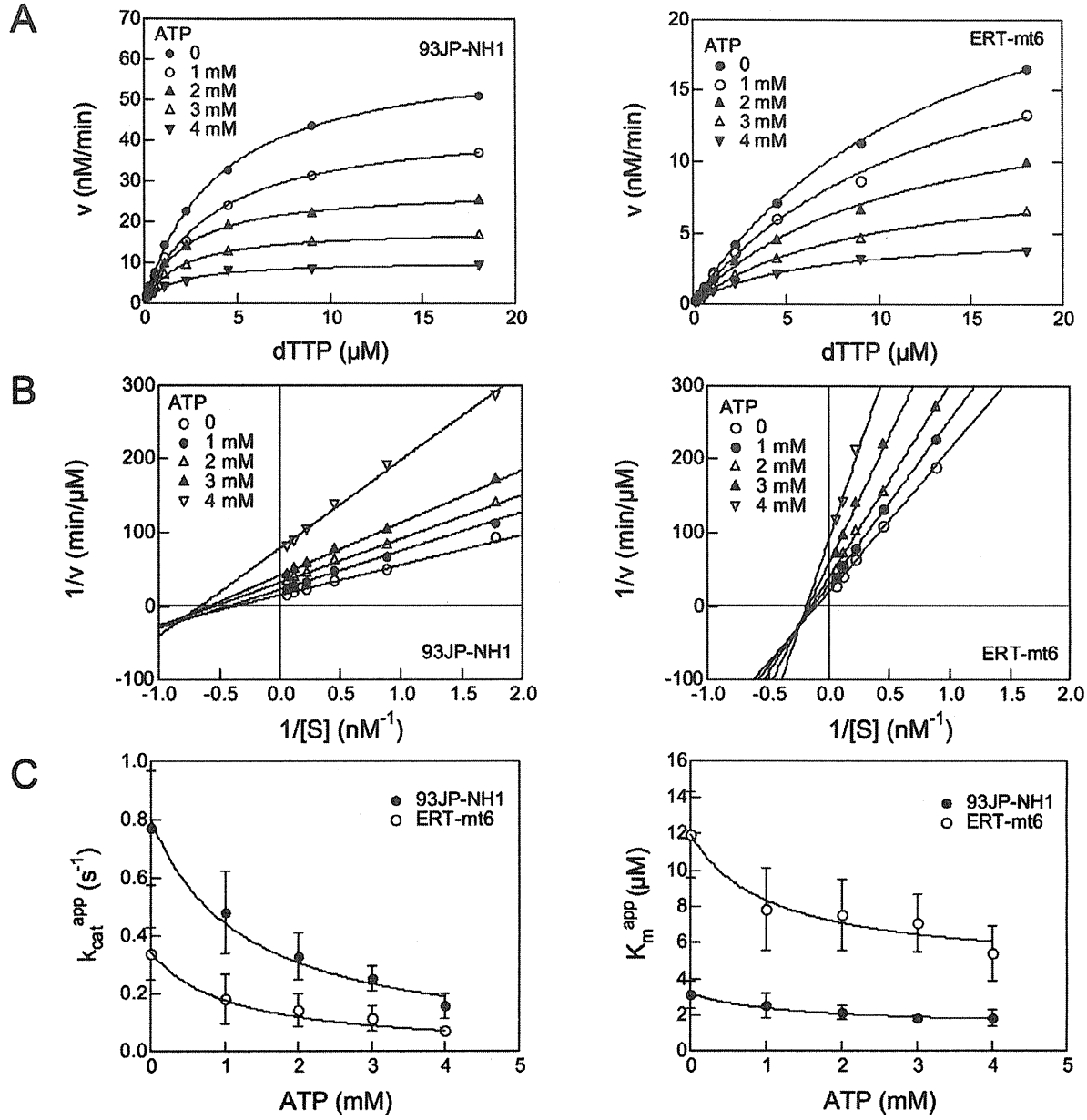

Figure 1. Effects of ATP on HIV-1 RT reaction kinetics. A. The substrate-velocity curves of purified HIV-1 RTs in the presence of ATP. RNA-dependent DNA polymerase activity [13] of the purified RTs was measured using various concentrations of [α-^{32}P]dTTP and poly (rA)·p(dT)$_{12-18}$ in the presence of ATP. Representative results with 93JP-NH1 RT (left) and ERT-mt6 RT (right) are shown. **B.** Lineweaver-Burk double-reciprocal plots for ATP-dependent inhibition of dTTP incorporation. Reciprocal values of the initial velocities and substrate concentrations in Figure 1A are plotted. **C.** Effects of ATP on K_m (left) and k_{cat} (right) values in RT reaction. The K_m and k_{cat} values were estimated by fitting of the initial velocity of dTTP incorporation to Equations 3 and 4 as described in Materials and Methods. The mean values with variances of the six independent experiments are shown.

doi:10.1371/journal.pone.0008867.g001

fingers-closed ternary, and pre-translocation complex stages [14] (Figure 3).

The 3-D models were used to search for a possible binding site for nucleotides by docking simulations [22]. A previous study suggested that incoming dNTP and NRTIs bind along the p66 fingers subdomain of the fingers-open ternary RT complex at the post-translocation stage [23] (Figures 3A and 3B), as is generally seen in other polymerases [24,25,26,27,28]. The binding position was in agreement with the biochemical mode of NRTI inhibition, competitive inhibition, as shown by our kinetic study of AZTTP (Figure S2) and previous studies [17,18]. This position was also consistent with the position needed to initiate the base pair formation at the enzyme active center after rotation (~20°) of the β3-β4 loops to form a fingers-closed ternary complex [5] (Figures 3B and 3C).

The 3-D models of pre- and post-translocation complexes corresponding to E and ES in the kinetic model (Figure 2C) were used to search for a possible binding site for the ATP molecule by docking simulations [22]. The simulations suggested that the ATP molecule could bind to the 93JP-NH1 and ERT-mt6 RTs at the pre-translocation (Figure 3D) and the post-translocation (Figure 3A) stages. The ATP molecule was predicted to bind